Report
R-20-04
October 2021

Assessment of complexing agent concentrations for the post-closure safety assessment in PSAR SFR

Miranda Keith-Roach
Maria Lindgren
Klas Källström

SVENSK KÄRNBRÄNSLEHANTERING AB

SWEDISH NUCLEAR FUEL
AND WASTE MANAGEMENT CO

Box 3091, SE-169 03 Solna
Phone +46 8 459 84 00
skb.se

SVENSK KÄRNBRÄNSLEHANTERING

ISSN 1402-3091
SKB R-20-04
ID 1888007
October 2021

Assessment of complexing agent concentrations for the post-closure safety assessment in PSAR SFR

Miranda Keith-Roach, Maria Lindgren
Kemakta Konsult AB

Klas Källström, Svensk Kärnbränslehantering AB

This report is published on www.skb.se

Abstract

Low- and intermediate-level radioactive waste produced in Sweden is disposed of in the repository for short-lived low- and intermediate-level waste (SFR). Complexing agents used at the nuclear sites are present in this waste and others will be generated in situ through the degradation of waste components such as cellulose. These may potentially reduce radionuclide sorption in the BMA, the silo and BTF vaults of SFR and enhance radionuclide transport to the geosphere. This report updates two previous assessments of complexing agents in SFR (Fanger et al. 2001, Keith-Roach et al. 2014). First, the literature is reviewed to a) identify the materials that are likely to degrade and produce complexing agents in situ, b) obtain data for the likely rates of relevant processes, and c) assess complexing agent and degradation product sorption to hydrated cement and their likely solubility and stability under repository conditions. The mass of different complexing agents and cellulose in each SFR waste type is then summarised using the most recent information from the nuclear sites and the latest Inventory report (SKB 2019). The concentrations of complexing agents have been calculated in each relevant waste type and larger part of SFR, e.g. 1BMA compartments, 2BMA caissons, the silo construction and BTF waste blocks, as well as each rock vault. In the case of the cellulose degradation product isosaccharinate (ISA), concentrations were calculated as a function of time. Sorption of ISA and gluconate to hydrated cement has been accounted for, as have the solubility limits of the α-diastereoisomer of ISA, citrate and oxalate in a cementitious system. All other complexing agents were assumed to be in solution. The results show that the complexing agents with the highest dissolved concentrations are ISA and nitrilotriacetate (NTA). Modelling in PhreeqC suggested that ISA is able to reduce the sorption of many radionuclide species under repository conditions, while NTA affects the sorption of tetravalent actinides and analogous species. Therefore, the concentrations of ISA and NTA were used to calculate sorption reduction factors for application in the radionuclide transport calculations in SR-PSU (PSAR).

Sammanfattning

Låg- och medelaktivt avfall som produceras i Sverige deponeras i slutförvaret för kortlivat radioaktivt avfall (SFR). I detta avfall förekommer komplexbildare, dels från produkter som används vid de kärntekniska anläggningarna, dels från avfallsmaterial såsom exempelvis cellulosa som bryts ner till komplexbildare över tid. Dessa komplexbildare kan potentiellt hämma radionuklidsorptionen i BMA- och BTF-salarna och silon i SFR och öka uttransporten av radionuklider till geosfären. Föreliggande rapport utgör en uppdaterad uppskattning av komplexbildare i SFR utifrån två tidigare rapporter (Fanger et al. 2001, Keith-Roach et al. 2014). I rapporten presenteras först en litteraturgenomgång för att a) identifiera vilka material som förväntas brytas ner och producera komplexbildare i avfallet, b) erhålla data för hastigheterna för dessa processer, och c) uppskatta komplexbildarnas och nedbrytningsprodukternas sorption till cement och förväntade löslighet och stabilitet under slutförvarsförhållanden. Mängderna av de olika komplexbildande materialen i SFR-avfallstyper har sammanställts med hjälp av den senaste informationen från de kärntekniska anläggningarna och den senaste inventarierapporten (SKB 2019). Utifrån mängderna har komplexbildarnas lösta koncentrationer beräknats, i kollin av respektive avfallstyp liksom i definierade delar av SFR såsom 1BMA-fack, 2BMA-kassuner, silokonstruktionen och BTF-avfallsdomäner, samt totalt i respektive förvarsdel. Gällande cellulosanedbrytningsprodukten isosackarinat (ISA) har koncentrationen beräknats som funktion av tid. ISAs och glukonats sorption till cement har beaktats, liksom α-ISAs, citrats och oxalats begränsade lösligheter i cementmiljö. Resterande komplexbildare antas vara fullständigt upplösta. Resultaten visar att av alla relevanta komplexbildare är ISA och nitrilotriacetat (NTA) de med den högsta lösta koncentrationen i SFR. Termodynamisk modellering med PhreeqC indikerar att ISA kan hämma många radionukliders sorption under slutförvarsförhållanden, medan NTA påverkar sorptionen av tetravalenta aktinider och analoger därav. De beräknade koncentrationerna av ISA och NTA har således använts för att härleda sorptionsreduktionsfaktorer för tillämpning i radionuklidtransportberäkningarna i SR-PSU (PSAR).

Contents

1 Introduction

Low- and intermediate-level radioactive waste produced in Sweden is disposed of in SFR. Complexing agents used at the nuclear sites are present in some wastes and other complexing agents will form in situ, notably isosaccharinate (ISA) during the alkaline degradation of cellulose. Organic cement additives may also have complexing properties. Since complexing agents may reduce radionuclide sorption to hydrated cement phases in the repository, they may affect the corresponding SFR safety function, called *good retention* in the F-PSAR version of the SR-PSU safety assessment and *sorb radionuclides* in PSAR. In the safety assessment, radionuclide sorption is calculated using K_d values, which assume that the ratio between solid and solution phase radionuclide concentrations is constant. Specific K_d values are defined for each radionuclide at each stage of cement degradation for implementation in the radionuclide transport modelling. It is important to assess the concentrations of complexing agents present in SFR to define the effect they are expected to have on the K_d values applied.

Previous studies (Fanger et al. 2001, Keith-Roach et al. 2014) have summarised the masses and concentrations of complexing agents anticipated in SFR. This report updates these estimates using the most recent waste inventory (SKB 2019), new assessments of detergent use at the nuclear sites, and the best available scientific understanding of cellulose degradation processes and complexing agent sorption to hydrated cement. This update of the report also presents sorption reduction factors (SRF) derived from the complexing agent concentrations, for specific groups of radionuclides in defined parts of SFR. The SRF will be applied in the radionuclide transport modelling of the safety assessment SR-PSU (PSAR).

2 Background information and literature review

This chapter revisits and updates the literature reviews in Fanger et al. (2001) and Keith-Roach et al. (2014). Comprehensive information on the effects of different complexing agents can be found mainly in two reports for the SR-PSU safety assessment: the Data report and the Waste and waste packaging process report, whose PSAR versions are still under development, although largely similar to the F-PSAR versions (SKB 2014a, b). The purpose of this chapter is to provide a broader understanding of the organic materials disposed of in SFR, the processes that affect solution-phase concentrations of potentially important complexing agents and the interactions of these potential complexing agents with radionuclides.

Inorganic ligands such as OH^-, CO_3^{2-}, NO_3^-, SO_4^{2-}, S^{2-}, PO_4^{3-}, CN^-, $B(OH)_4^-$, F^-, I^-, Cl^- and Br^- will also be present in the surrounding groundwater and/or the waste. Under the cementitious conditions of SFR, OH^- is expected to be the most important inorganic ligand in terms of radionuclide speciation and solubility. It has been concluded that, under these conditions, only cyanide complexes are of further importance for radionuclide (Ni, Ag, Pb) sorption (Bradbury and Van Loon 1997). However, cyanide present as the hexacyanoferrate anion ($Fe(CN)_6^{4-}$) forms weak complexes with metal cations (Bradbury and Van Loon 1997). Inorganic ligands are not considered further in this report.

2.1 Potential organic complexing agents present in SFR

A wide range of materials are present in the waste, packaging, backfill and construction of SFR (Appendix 1). These include a variety of organic complexing agents that are present in the waste from the detergents and chemicals used at the nuclear power plants, such as EDTA (ethylenediaminetetraacetate), NTA (nitrilotriacetate), NKP (sodium capryliminodipropionate), citrate, oxalate and gluconate (Figure 2-1). A small mass of picolinate was used in 1998 (Fanger et al. 2001) but there is no evidence to suggest it was used for a long time, based on Keith-Roach et al. (2014) and new information provided for this report (see Appendix 2). Picolinate is therefore not considered relevant for the safety of SFR.

Organic waste materials are also present that may degrade over time to form complexing agents, and organic cement additives may also degrade and/or leach. For clarity, all materials present in SFR are listed in Appendix 1 and for those not included in the discussion of degradation processes and degradation products in Section 2.2, a brief comment is given as to why.

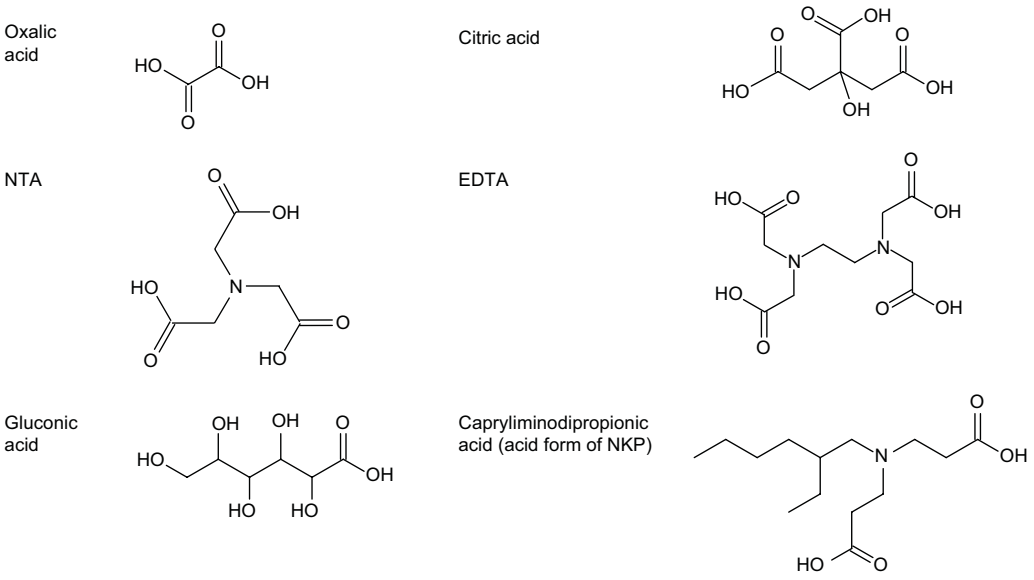

Figure 2-1. *Chemical structures of the acid forms of the main complexing agents present in SFR wastes.*

2.2 Degradation of organic material and products

The current understanding of the degradation processes affecting cellulose, lignin, polyacrylonitrile filter aids, bitumen, ion exchange resins, plastic and rubber, and cement additives is described in brief in Sections 2.2.1 to 2.2.7. Degradation of complexing agents that are disposed of in the waste or form in situ are discussed in Section 2.3.1.

2.2.1 Cellulose

Degradation mechanisms

Substantial amounts of cellulosic materials such as paper, textiles and wood can be present in low- and intermediate-level radioactive wastes. Under the highly alkaline conditions of a cementitious repository, cellulose degrades to water-soluble, low molecular weight compounds. The mechanisms and rates of alkaline cellulose degradation have been investigated in a number of studies (e.g. Glaus and Van Loon 2008, Pavasars 1999, Van Loon and Glaus 1998, Bradbury and Van Loon 1997).

The chemical structure of cellulose is shown in Figure 2-2. Cellulose degrades through the "peeling off" reaction under alkaline conditions. In this reaction, reducing end groups of the cellulose polysaccharide chain isomerise into reactive interim products that are then eliminated from the chain (Van Loon and Glaus 1998). The reaction produces new reducing end groups for further reaction, leading to stepwise elimination of glucose units and depolymerisation of the chain. The reaction sequence stops when the reactive interim product is converted to a stable meta-saccharinic end group on the polysaccharide chain, or a crystalline (inaccessible) region of the chain is reached. These two stopping reactions are termed the chemical stopping reaction and the physical stopping reaction, respectively. Once all end groups are stable or inaccessible, the peeling off reaction depends on the formation, or increased accessibility, of reducing end groups. The possible reaction mechanisms for this are termed "mid-chain scission", which involves alkaline hydrolysis of glycosidic bonds in the polymeric chain, and "decelerated peeling", which involves a dynamic equilibrium between crystalline and amorphous structures of cellulose (Glaus and Van Loon 2008).

Degradation products

The products of alkaline cellulose degradation depend on the composition of the surrounding solution (Bradbury and Van Loon 1997, Van Loon and Glaus 1997). In the presence of Ca^{2+}, as found in cement pore waters, the formation of ISA (Figure 2-2) is favoured with a typical yield of ~ 80 % (Bradbury and Van Loon 1997, Van Loon and Glaus 1997, Pavasars et al. 2003, Glaus and Van Loon 2008). The α- and β-diastereoisomers of ISA are formed in approximately equal proportions (Van Loon et al. 1999a). α-ISA exhibits particularly strong complexing properties and is therefore of most concern in terms of its potential to enhance radionuclide mobility (Pavasars 1999, Glaus et al. 1999, Van Loon et al. 1999b). Minor degradation products comprise short chain aliphatic carboxylates such as formate, acetate and lactate (Glaus et al. 1999, Van Loon et al. 1999a).

The overall chemical formula of cellulose is $(C_{12}O_{10}H_{20})_n$, although the reactive end group has the formula $C_6O_6H_{11}R$. The equation for the production of ISA in each step of the peeling off process is as follows:

$$C_6O_6H_{11}R + OH^- \rightarrow C_6O_6H_{12} + OR^- \qquad \text{Equation (2-1)}$$

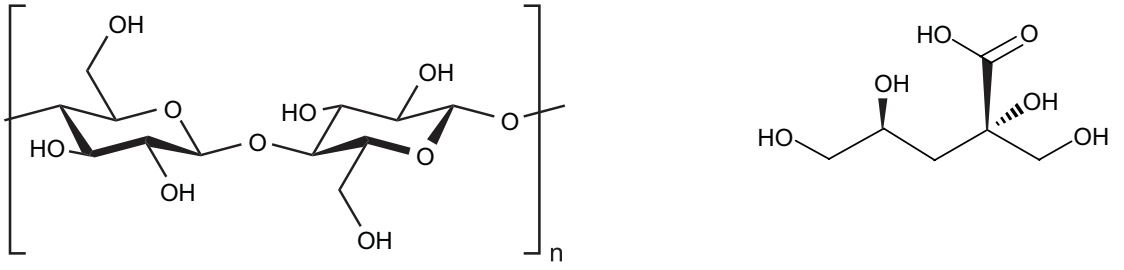

Figure 2-2. *Chemical structures of cellulose and ISA.*

Since the hydroxide ion that attacks the cellulose is incorporated into the ISA molecule that is peeled off, 162 g of the original cellulose ($C_6O_5H_{10}$) is degraded per mole of ISA produced.

Degradation rates

Cellulose degradation rates reported in the literature vary according to the cellulosic material and experimental conditions used. Different types of cellulose are polymerised to different degrees and this affects the mole fraction of reducing end groups initially present in the material, i.e. available for reaction. The pH, cations present, temperature and redox conditions are important (Pavasars 1999, Van Loon and Glaus 1997, Glaus and Van Loon 2009). Irradiation can also enhance alkaline degradation of cellulose (Nixon et al. 2017), but this has only been studied at higher doses than found or expected in SFR.

Most experiments have been performed for a limited period of time or at high temperatures, and extrapolation of the results to repository conditions and timescales has generated contrasting conclusions. However, Glaus and Van Loon (2008) studied the degradation of four cellulosic materials under artificial cement porewater conditions over a 12-year period, the longest study to date. Their data for Tela tissue degradation are therefore considered here to be the most relevant and complete data for predicting cellulose degradation in SFR, and are applied throughout this report. Glaus and Van Loon (2008) presented two equations to describe cellulose degradation, the first using mid-chain scission to control the long-term degradation rate and the second using decelerated peeling. They argued that decelerated peeling is the more likely mechanism. However, the equation given for decelerated peeling is zero order and so does not account for the decrease in the concentration of cellulose over time, while the equation involving mid-chain scission does. Therefore, the equation for the mid-chain scission reaction (Glaus and Van Loon 2008; shown here as Equation (2-2)) has been used to estimate the degree of cellulose degradation over time.

$$(\text{celdeg})_t = 1 + e^{-k_h t}\left[\frac{k_1}{k_t} \times (G_r)_0 \times \left(1 - e^{-k_t t}\right) - 1\right] \qquad \text{Equation (2-2)}$$

where

$(\text{celdeg})_t$ = fraction of cellulose degraded as a function of time

k_h = product of the average number of peeled glucose units and the intrinsic reaction rate constant for the mid-chain scission reaction

k_1 = first order rate constant for the propagation of the peeling off reaction

k_t = first order rate constant for the stopping reaction

$(G_r)_0$ = initial mole fraction of reducing end groups

Glaus and Van Loon (2008) determined the following reaction rate constants for Tela tissue degradation by best fit to their experimental data:

$k_h = (1.0 \pm 0.2) \times 10^{-7}\ h^{-1}$

$k_1 = (1.0 \pm 0.1) \times 10^{-2}\ h^{-1}$

$k_t = (2.9 \pm 0.5) \times 10^{-4}\ h^{-1}$

The degree of polymerisation of a material has an inverse relationship with the initial mole fraction of reducing end groups ($(G_r)_0$), and this generated a $(G_r)_0$ value of 9.0×10^{-4} for Tela tissue.

The experimental data showed a rapid initial degradation rate and > 3 % of the cellulose in Tela tissue degraded over the first 2 years. The remaining cellulose then degraded more slowly; Equation (2-2) calculates that cellulose degradation will be virtually complete (~99 %) after 5 000 years. Similarly, using the rate constants and $(G_r)_0$ values given in Glaus and Van Loon (2008) for paper, the cellulose in paper will be almost completely degraded (~100 %) after 5 000 years. The experimental data and associated constants derived for cotton suggest that cotton degradation will be slower, with ~76 % degraded after 5 000 years, and ~99 % after 25 000 years.

2.2.2 Lignin

Lignin is a highly complex polymer based on aromatic alcohols. As reviewed by Klapiszewski et al. (2017), alkaline degradation of lignin has been studied under optimised laboratory conditions in order to understand its structure. The functional groups of the degradation products of lignin in general, and of the alkaline degradation products of lignin specifically, include benzene rings, alcohols, ketones and ethers. The high stability of lignin and the lack of functional groups that are associated with high complexing power, such as carboxylic acids, suggest that lignin is not of concern in SFR.

2.2.3 Filter aids

Filter aids are used to reduce the clogging of filters and thus improve filtration. They are finely divided solid materials and the most common products are based on inorganic perlite and diatomaceous earth. However, organic filter aids based on polyacrylonitrile (PAN) fibres with a chemical formula of $[C_3H_3N]_n$ are also used at Forsmark and Oskarshamn nuclear power plants and Clab. UP2 is an example of this type of product.

The PAN structure has been found to undergo relatively small changes in an experiment simulating its use at a nuclear site, altering from an isotactic to syndiotactic structure (Duro et al. 2012). During alkaline degradation, nitrile groups are slowly hydrolysed to amides and carboxylic acids (e.g. Ermakov et al. 2000), with carboxylic acids being the likely final product. Depolymerisation or other reactions generating low molecular units will also take place; Duro et al. (2012) found that soluble UP2 degradation products were a mixture of carboxylic acids, amides, alkenes and ketones. However, only a limited proportion of the degradation products were characterized in this study (8 and 28 % at pH 12.5 and 13.4, respectively).

The rate of UP2 degradation has been investigated under alkaline conditions (Dario et al. 2004, Duro et al. 2012, Holgersson et al. 2011). Duro et al. (2012) showed that temperature and pH have a very clear influence on the rate of degradation and the lowest rates of degradation were found at pH 12.5 compared to pH 13.4, and room temperature compared to 60 °C. The dissolved organic carbon (DOC) concentration increased rapidly in the early part of the experiments. The rate of degradation then decreased progressively over time. At pH 12.5, the DOC concentration was about 8 mg/L by 694 days, and the increase from 276 days to 694 days was small (1.2 mg/L DOC). The DOC concentration can be compared with the initial UP2 concentration of 25 g/L in the experiments. The study by Holgersson et al. (2011) determined higher DOC concentrations over time with a similar initial UP2 concentration (24 g/L) and the DOC concentration reached ~150 mg/L at pH 13.4 and ~45 mg/L at pH 12.5 after about 3.3 years. The experimental data were however too few to determine how the rate changes over time and whether degradation had reached a plateau.

UP2 from Forsmark is conditioned in bitumen (waste type F.17) prior to disposal, which is likely to delay the onset of alkaline degradation for some time. Therefore, degradation is expected to take place at pH 12.5 (portlandite-buffered conditions) or less and the available experimental evidence suggests that this will limit degradation. F.17 wastes are disposed of in 1-2BMA.

PAN filter aids used at Oskarshamn are dewatered and disposed of in concrete tanks (waste type O.07, allocated to the silo), while those used at Clab are cement-solidified in concrete moulds (waste type C.02, allocated to 1–2BTF). Both of these PAN filter aids are therefore expected to be exposed to pH 13.4 conditions and degrade extensively. Further experiments are being carried out to investigate the degradation of PAN filter aids and the implications of this for radionuclide sorption.

2.2.4 Bitumen

Bitumen is a mixture of high molecular weight aliphatic and aromatic hydrocarbons, and smaller amounts of compounds that contain nitrogen, oxygen and sulfur (Allard and Persson 1985). It is therefore expected to change chemically over time under oxidising conditions. However, according to the Waste form and packaging process report for the safety assessment SR-PSU (SKB 2014b), degradation of bitumen will be very slow under anaerobic, low-flow and high-pH conditions. These conditions will prevail for a considerable period of time in the long-term safety analysis.

The chemical products of bitumen degradation under oxic conditions are reported to have weak or negligible complexing power and will have no significant influence on the sorption of radionuclides onto cementitious materials (Pettersson and Elert 2001). The dissolved concentrations of organic substances and trace elements were not elevated in the alkaline groundwater from a site in northern Jordan with natural occurring bitumen (SKB 1991). Therefore, bitumen is not considered to be of concern in SFR with regard to the formation of complexing agents.

2.2.5 Ion-exchange resins

Ion-exchange resins used at the Swedish nuclear sites consist of polystyrene chains with amine functional groups in anion exchangers and sulfonic acids in cation exchangers (Allard and Persson 1985). Low sulfur cation exchange resins are also used, which have carboxylate functional groups on a polyacrylate support (Allard et al. 2002). Radiolysis of cation- and anion-exchange resins under alkaline conditions (0.05 M NaOH, initial pH ~12.7), with an absorbed dose of 1.7 MGy, was found to produce oxalate (Van Loon and Hummel 1999a) and amines (Van Loon and Hummel 1999b), respectively, among the degradation products. However, chemical degradation was not observed under equivalent alkaline conditions in 10-day experiments without irradiation. Allard et al. (2002) also concluded that possible degradation products of a mixed bed ion-exchange resin would not reduce radionuclide sorption.

Rébufa et al. (2015) investigated radiolytic degradation of ion exchange resins as a function of absorbed dose from an external gamma source and under different conditions. In an anaerobic/water atmosphere, radiolysis of a mixed bed resin was observed at absorbed doses ≥ 3 MGy. However, the waste acceptance criteria for organic-material-containing wastes in 1BMA and the silo is 0.1 MGy[1]. Radiolysis of ion-exchange resins is therefore not expected in SFR. In any case, radiolytic degradation products have been shown to have a negligible influence on the sorption of radionuclides to cementitious materials (Bradbury and Sarott 1994, Bradbury and Van Loon 1997, Allard and Persson 1985). Ion-exchange resins are not considered to be of concern in SFR with regard to the formation of complexing agents.

2.2.6 Plastic and rubber

Plastic and rubber can be divided into two categories according to the polymerisation reaction used in their production:

1. Addition polymers, e.g. polyethylene ($(C_2H_4)_n$), polystyrene ($(C_8H_8)_n$), polyvinyl chloride (PVC, $(C_2H_3Cl)_n$) and polyisoprene found in rubber ($(C_5H_8)_n$).
2. Condensation polymers e.g. polyesters (e.g. PET) and polyamides (e.g. Nylon).

Addition polymers contain only C atoms in the polymeric backbone (Van Loon and Hummel 1995). The C–C backbone is therefore generally very strong and insensitive to alkaline degradation. Dawson (2013a) irradiated low density polyethylene in a saturated $Ca(OH)_2$ solution using an external gamma source up to a maximum absorbed dose of 10 MGy. Irradiation had no systematic effect on the total organic carbon (TOC) concentration of the solution, which varied between 5–12 mg/L. GC–MS analysis of the solution phase identified negligibly low concentrations of a potential complexing agent, benzene dicarboxylic acid, and long chain alkanes. The information available suggests that neither alkaline nor radiolytic degradation of polyethylene, or other addition polymers, will occur significantly in SFR. Addition polymers are an important component of plastic waste in nuclear facilities (Filby et al. 2016).

In condensation polymers, functional groups provide the links between the monomers. The ester or amide functional groups involve electron withdrawing groups that result in a slightly positively charged C atom. This creates a point for nucleophilic attack by hydroxide ions, and condensation polymers are therefore prone to alkaline hydrolysis of the polymeric chain (Van Loon and Hummel 1995). Hydrolysis is essentially the reverse of the condensation reaction used to form the polymer. The alkaline degradation of polyamides produces dicarboxylic acids and diamines (or in some cases carboxylic acids and amines of higher order), while alkaline degradation of polyesters produces

[1] **Lihnell M, Södergren K, 2018.** Acceptanskriterier för avfall i SFR1. SKBdoc 1336074 ver 3.0, Svensk Kärnbränslehantering AB. (In Swedish.) (Internal document.)

dicarboxylic acids and diols. High concentrations of dicarboxylic acids could influence radionuclide sorption, and could therefore be important, especially within individual waste packages. However, as a range of plastics and rubber with different chemical structures are disposed of in SFR, the concentrations of individual condensation polymer degradation products are considered unlikely to be important at the compartment or vault scale of SFR.

PVC contains non-polymeric plasticiser molecules that can comprise a significant proportion of the total mass (Baston et al. 2017). Baston et al. (2017) investigated the degradation products of commercial PVC film and three phthalic acid ester plasticisers that were irradiated using an external gamma source at different temperatures in saturated $Ca(OH)_2$ solution. The phthalic acid esters underwent de-esterification to phthalate and alcohols. However, GC–MS analysis identified phenols as the main dissolved organic species arising from the irradiation of commercial PVC under alkaline conditions. As the phenols did not arise from the polymer chain or the plasticisers, they were thought be derived from other additives in the PVC, potentially triphenyl phosphate. PVC degradation products were found to influence the sorption of Pu(VI) and U(VI). However, the authors of the study were not able to identify the organic species responsible and they concluded that the effect was small in comparison to the effect of cellulose degradation products (Baston et al. 2017). Modelling studies have shown that Ni, Eu and Am (Garcia et al. 2018) and Pu(VI) and U(VI) (Baston et al. 2017) are not complexed by phthalate under alkaline conditions, even though phthalate is an important complexing agent under near neutral conditions (Garcia et al. 2018).

Rubber also contains additives, including phthalate ester plasticisers (Filby et al. 2017). Long chain alkanes and *N*-methylaniline ($C_6H_5NH(CH_3)$) were seen to diffuse out of neoprene under alkaline conditions. When the samples were also irradiated using an external gamma source to an absorbed dose of 0.15 MGy, *N*-methyl-aniline became the main degradation product identified (Dawson 2013b). The compounds identified comprised a very small proportion of the total organic carbon detected by UV analysis. Overall, the mass of total organic carbon determined was a very low proportion of the total mass of neoprene and the compounds identified are not expected to complex radionuclides.

Overall, although plastic and rubber are important organic constituents of SFR waste, they are either expected to be resistant to alkaline degradation or to degrade to organic molecules with no or a relatively low ability to complex radionuclides. The effect of additives in PVC and rubber on radionuclide sorption is also expected to be negligible.

2.2.7 Cement additives

Cement additives are used to improve the characteristics of cement paste during casting and/or to impart good long-term properties to the hardened material, such as a low porosity. The products available have changed and improved over time and a range of different terms are used to describe cement additives according to their function. Examples include cement grinding agents, used in the production of the cement, retarders, which reduce the rate of setting, and superplasticisers, which improve the workability of cement at low water:cement clinker ratios. The concrete developed for the 2BMA caissons, for example, contains two superplasticisers (MasterGlenium Sky 558 and MasterSure 910) and a retarder (MasterSet RT 401) (Lagerblad et al. 2017). Cement grinding agents are present in cement products, but in relatively low amounts (Keith-Roach and Höglund 2018).

Examples of organic cement additives used or planned for use in SFR are given in Table 2-1. It should be noted that a wide range of cements and concretes with different cement additives have been used over time, in different parts of SFR and at the nuclear power plants. Therefore, it is not possible to map the masses of individual cement additives present in SFR. The content of commercial products is proprietary information, thus products can contain a range of unknown or undefined components. This further complicates identification of the compounds present in SFR.

Cement additives are based on a range of compounds with different degradation rates and products. Retarders can be composed of organic and inorganic material. The organic components can include lignosulfonates, hydroxycarboxylic acids, and carbohydrates (Hakanen and Ervanne 2006).
As shown in Table 2-1, MasterSet RT 401 contains sucrose. Sucrose has been seen to undergo alkaline hydrolysis at 100 °C to form hydroxyacetone, 2-hydroxy-3-methyl-2-cyclopenten-1-one, 2,5-dimethyl-4-hydroxy-3(2H)-furanone, acetate, propionate and lactate (Shaw et al. 1969). These molecules are not expected to form strong complexes with radionuclides.

Table 2-1. Examples of cement additives present in SFR.

Additive	Composition	Comment	Examples of amounts used	Reference for mass used
Cement grinding agents	E.g. propylene glycol, diethylene glycol, triethanolamine, polycarboxylate ethers		50–200 g/t cement	Keith-Roach and Höglund (2018)
MasterSet RT 401(Retarder)	Sucrose		0.96 kg/m^3 in 2BMA caisson construction concrete (planned)	Lagerblad et al. (2017)
Cementa Flyt M97, PA in Betokem (superplasticisers)	Lignin, lignosulfates, lignin sulfonates	Not considered to be cellulosic due to structural differences. This is a change from Fanger et al. (2001)	1 000 kg in SFR	Fanger et al. (2001)
Sikament 10 (superplasticiser)	Vinyl maleinic acid copolymer		6 kg/waste package for several R.10 variants and 17 kg/waste package for R.15/R.16 050 produced before 97/03/03. There was also 15–25 kg in the stabilised R15/R16 waste produced before 97/03/03	Reported to SKB by Ringhals
Methocel (superplasticiser)	Regarded as cellulose	Used in the silo and included in estimation of the silo's ISA concentration	5 200 kg in the silo	Fanger et al. (2001)
Peramin F and L (superplasticisers)	Melamine sulfonate polymer with formaldehyde		Peramin L used in O.07 and O.08 concrete packaging (0.2 % of cement)	Andersson (2015)[2] Granflo (2015)[3]
Barra 55 (superplasticiser)	"Vinsolharts"/ lignin sulfonate		Small amounts in SFR	Fanger et al. (2001)
Sikament 210, Mighty 150, Melcrete (superplasticisers)	Naphthalenesulfonic acid polymer with formaldehyde		Melcrete is used in O.07 and O.08 concrete packaging, added at 1 % of cement weight	Andersson (2015)[2] Granflo (2015)[3]
Peramin Conpac 30	Polyether polycarboxylate		Has been used in O.07 and O.08 concrete packaging, added at 0.65 % of cement weight	Andersson (2015)[2] Granflo (2015)[3]
Sika ViscoCrete-125 and 225	Polycarboxylate		Used in the lids of O.07 and O.08	Andersson (2015)[2]
MasterGlenium Sky 558, MasterSure 910	Polycarboxylate ether		Combined use: 3 kg/m^3 in 2BMA caisson construction concrete (planned)	Lagerblad et al. (2017)

Superplasticisers are based on lignin, cellulose, vinyl maleic acid co-polymers, melamine sulfonate polymers, naphthalene sulfonic acid polymers, and polyether carboxylates. The chemical building blocks for these polymers are shown in Table 2-2.

The recent review in Keith-Roach and Höglund (2018) provides information on how superplasticisers bind to cement, leach, degrade and affect radionuclide sorption. In brief, superplasticisers sorb strongly to cement particles and lower the rate of particle coagulation through either steric hindrance or charge repulsion. This increases the workability of the cement paste without compromising on the quality of the final concrete, for example by using larger amounts of water. Leaching studies show that oligomers, dimers, monomers and unreacted precursor molecules are present in the porewater and leach from newly cast HCP, rather than the polymers themselves (Ruckstuhl et al. 2002, Herterich et al. 2003, Yamamoto et al. 2008). Polyethylene glycol (PEG) sidechains of polycarboxylate superplasticisers have also been seen in the leachate (Herterich et al. 2004), and the ester group linking the PEG to the

[2] **Andersson K, 2015.** Sammanställning av kemikal ier och komponenter i avfallsemballage av betong samt redovisning av beräkning för stapelbarhet för betongkokiller. Reg nr 2015-15867 utgåva 2.0, OKG AB. SKBdoc 1518979 ver 1.0, Svensk Kärnbränslehantering AB. (In Swedish.) (Internal document.)

[3] **Granflo T, 2015.** Brevsvar angående mail daterat 2015-04-29. Reg Nr 2015-21475, Nordiska VA-Teknik AB. SKBdoc 1585568 ver 1.0, Svensk Kärnbränslehantering AB. (In Swedish.) (Internal document.)

polymeric backbone is a relatively labile bond. PEG is not of concern with respect to radionuclide complexation. It is difficult to differentiate degradation products from the non-polymeric components of the superplasticiser product.

Glaus et al. (2006) examined changes in superplasticiser components in the solid phases and porewater over 20 months and found that the compounds in the porewater changed while those associated with the solid phase did not. In the long term, release of the superplasticiser will require scission of the polymer backbone and/or changes in the cement phases present (Keith-Roach and Höglund 2018). Keith-Roach and Höglund (2018) did not find any evidence for the abiotic degradation of polycarboxylate or polynaphthalene backbones.

Table 2-2. Chemical building blocks of relevant polymers (adapted from Keith-Roach and Höglund 2018).

Name	Structure
Acrylic acid (prop-2-enoic acid)	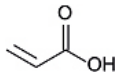
Ether (ethoxyethane)	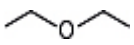
Cellulose	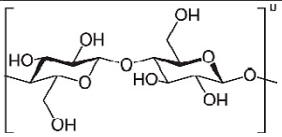
Formaldehyde (methanol)	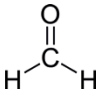
Lignosulfonate Figure reproduced from Altwaiq et al. (2020) with permission under Creative Commons Attribution International License (http://creativecommons.org/licenses/by/4.0/).	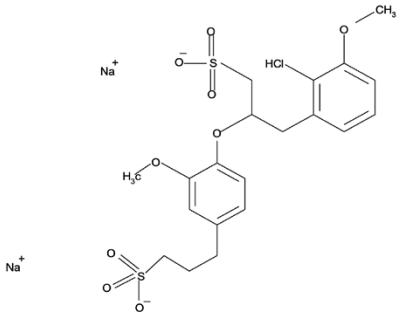
Maleic acid ((2Z)-but-2-enedioic acid)	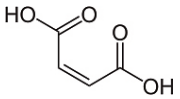
Melamine (1,3,5-triazine-2,4,6-triamine)	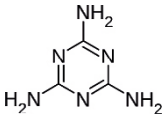
Methacrylic acid (2-methylprop-2-enoic acid)	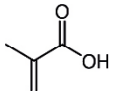
Naphthalene	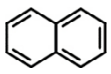
Sulfonate functional group (attached to an organic group, “R”)	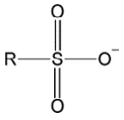
Vinyl functional group	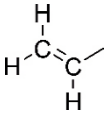

2.3 Behaviour and impact of complexing agents

Complexing agents affect the safety of a low- or intermediate-level waste repository if they are stable, dissolved and able to affect the sorption of radionuclides under the prevailing geochemical conditions. These issues are reviewed in this section for the degradation products identified in Section 2.2 that are potentially of concern for SFR (ISA, PAN degradation products, superplasticiser degradation products) and common decontamination agents (i.e. EDTA, NTA, citrate, oxalate and gluconate) used at the NPPs.

2.3.1 Degradation of complexing agents, precipitation and sorption to hydrated cement

Although most complexing agents undergo chemical or biological degradation under aerobic conditions, their degradation under anaerobic, highly alkaline conditions is less well defined. ISA degradation has, however, been studied in a suite of relevant long-term (hundreds of days) experiments (Glaus and Van Loon 2009). Within the experimental errors, there was no evidence to suggest that ISA degraded under conditions representative of a cementitious repository (Glaus and Van Loon 2009). This is consistent with the results of cellulose degradation experiments in which ISA was found to be present at a constant proportion of the total dissolved organic carbon under artificial cement porewater conditions over a period of 12 years (Glaus and Van Loon 2008). Significant microbial degradation of ISA is not expected in repository environment until late stages of cement degradation, because a high pH (> 12) limits microbial processes, including ISA degradation by alkaliphilic bacteria (Rizoulis et al. 2012). Therefore, for this report, ISA degradation has not been considered. Since the degradation of other complexing agents has not been demonstrated under repository conditions, they are also assumed to be stable for the purposes of this report.

The dissolved concentrations of complexing agents may also be affected by precipitation and/or sorption to available hydrated cement. Precipitation can be important for oxalate, citrate and the α-diastereoisomer of ISA in a cementitious repository, due to their relatively low solubility products with Ca^{2+}. Oxalate concentrations are expected to be limited to $\leq 10^{-5}$ M (Van Loon and Hummel 1995), while dissolved α-ISA concentrations have been calculated to be limited to 0.02 M during the portlandite phase of cement degradation (0.02 M Ca^{2+}; 0.05 M ionic strength) (Van Loon and Glaus 1998). The α-diastereoisomer of ISA has the greater ability to complex radionuclides (Pavasars 1999, Glaus et al. 1999, Van Loon et al. 1999b) and therefore the solubility of this isomer is most relevant. The PhreeqC calculations in Appendix 3 suggest that precipitation of calcium citrate will limit citrate concentrations to about 1 mM in SFR.

Sorption of ISA and gluconate to hydrated cement has been well characterised for the early stages of cement degradation, and the sorption isotherms can be used to estimate solution phase concentrations of these complexing agents in a repository. Experiments have shown that hydrated cement can sorb up to 0.3 moles of ISA per kg of hydrated cement (Van Loon et al. 1997, Van Loon and Glaus 1998) or 0.74 mole gluconate per kg hydrated cement (Glaus et al. 2006). ISA and gluconate may compete for the same sorption sites, and this needs to be considered if wastes contain both cellulose and gluconate at high concentrations relative to cement.

Van Loon et al. (1997) presented two different sorption isotherms for estimating the sorption of ISA to hydrated cement (Equation (2-3) and Equation (2-4)). The non-linear two-site model (Equation (2-4)) was found to be the better isotherm for ISA (Van Loon et al. 1997). The parameter values given are for pH 13.3. α- and β-ISA show comparable sorption isotherms (Van Loon and Glaus 1998).

$$[\mathrm{ISA}]_{\mathrm{sorbed}} = \frac{K \times q \times (\mathrm{ISA})_{\mathrm{eq}}}{1 + K \times (\mathrm{ISA})_{\mathrm{eq}}} \qquad \text{Equation (2-3)}$$

where

$[\mathrm{ISA}]_{\mathrm{sorbed}}$ = sorbed concentration of ISA at equilibrium (mol kg^{-1})

K = adsorption-affinity constant = 286 L mol^{-1}

q = adsorption capacity of the hydrated cement for ISA = 0.17 mol kg^{-1}

$(\mathrm{ISA})_{\mathrm{eq}}$ = solution phase concentration of ISA at equilibrium (M)

$$[\mathrm{ISA}]_{\mathrm{sorbed}} = \frac{K_1 \times q_1 \times (\mathrm{ISA})_{\mathrm{eq}}}{1 + K_1 \times (\mathrm{ISA})_{\mathrm{eq}}} + \frac{K_2 \times q_2 \times (\mathrm{ISA})_{\mathrm{eq}}}{1 + K_2 \times (\mathrm{ISA})_{\mathrm{eq}}}$$ Equation (2-4)

where

K_1 = adsorption-affinity constant of site 1 = 1 730 L mol^{-1}

q_1 = adsorption capacity of site 1 = 0.1 mol kg^{-1}

K_2 = adsorption-affinity constant of site 2 = 12 L mol^{-1}

q_2 = adsorption capacity of site 2 = 0.17 mol kg^{-1}

Tasi (2018) studied the sorption of ISA to a cement relevant to SFR at pH ~12.5 and found that the two-site model (Equation (2-4)) was also most suitable at this pH. A higher degree of sorption was observed than in Van Loon et al. (1997), which is consistent with maximum ISA sorption to cement occurring at pH 12.6 (Pointeau et al. 2008). The parameter values for binding site 1 were accordingly higher (K_1 = 2 510 L mol^{-1}, q_1 = 0.18 mol kg^{-1}), although the values for site 2 were the same as in Van Loon et al. (1997).

Gluconate sorption is also described by Equation (2-4), with

$K_1 = (2 \pm 1) \times 10^6$ L mol^{-1}

$q_1 = 0.04 \pm 0.02$ mol kg^{-1}

$K_2 = (2.6 \pm 1.1) \times 10^3$ L mol^{-1}

$q_2 = 0.7 \pm 0.3$ mol kg^{-1} (Glaus et al. 2006)

The sorption of other complexing agents to hydrated cement has not been studied to the same degree, and sorption isotherms are not available. Sorption of all complexing agents other than ISA and gluconate is therefore assumed to be zero in this report. There is, however, evidence that EDTA shows an affinity for degraded cement (Pointeau et al. 2008), and that NTA and citrate may show some affinity for hydrated cement (Dario et al. 2004).

2.3.2 Impact of complexing agents on radionuclide solubility and sorption

This section provides an overview of results from experimental and theoretical studies investigating the impact of complexing agents on the solubility of radionuclides and radionuclide sorption to relevant solid phases. The individual references have not been evaluated in detail.

Impact of ISA on radionuclide solubility

ISA is known to enhance the solubility of trivalent, tetravalent and, to a lesser extent, divalent ions. At pH 12, the solubility of Pu(IV) has been found to increase significantly with ISA concentrations above 1×10^{-5} M; changing the ISA concentrations from 1×10^{-3} to 5×10^{-3} M increased the solubility of Pu from ~10^{-5} to ~10^{-4} M (Greenfield et al. 1997). Tasi (2018) found that, at pH 12, $CaPu(OH)_3ISA_{-2H(aq)}$ was the dominant solution phase Pu(IV) species. The solubility of Pu(IV) was therefore affected by both the ISA and Ca^{2+} concentrations in experiments. An ISA concentration of 2×10^{-3} M has also been found to increase the solubility of U(IV), Th(IV) and Pu(IV) by factors of 250, 500 and 2×10^5 respectively (Allard et al. 1995).

Stability constants for the predominant actinide(IV)-ISA species that form under alkaline conditions have been derived from experiments. Examples include the ISA species of Th(IV) (e.g. Rai et al. 2009, Colàs 2014), U(IV) (e.g. Warwick et al. 2004, Kobayashi et al. 2019), Np(IV) (e.g. Rai et al. 2003) and Pu(IV) (e.g. Rai and Kitamura 2017). The speciation and solubility of Ni(II) is also affected by ISA (Warwick et al. 2003, González-Siso et al. 2018), but the effect on Ni(II) solubility is relatively small at the expected solubility limit for ISA in SFR of ~0.02 M ISA (González-Siso et al. 2018).

A recent study showed that both Eu(III) and Sr(II) can co-precipitate with Caα-ISA_2, which was considered to contribute to reduce radionuclide mobility in repositories where Caα-ISA_2 exceeds its solubility product (Chen et al. 2019). The maximum incorporation of Eu and Sr was found to be $Ca_{0.986}Eu_{0.014}(ISA)_2$ (2.4 % $Eu(ISA)_3$ by mass) and $Ca_{0.98}Sr_{0.02}(ISA)_2$ (2.2 % $Sr(ISA)_2$ by mass).

Impact of ISA on radionuclide sorption to cement

Sorption of ISA onto hydrated cement will affect its ability to enhance radionuclide solubility (Holgersson 2000) and experimental results are therefore influenced by the solid:solution ratio of the experiment, as well as the solid phase used. Therefore, comparability between experimental results is only expected if the same solid:solution ratio was applied or the concentration of ISA remaining in the solution phase was reported. Van Loon and Glaus (1998) used feldspar specifically to avoid the complications of ISA sorption to the experimental solid phase. Furthermore, whether enantiomerically mixed ISA or pure α-ISA is used may affect the impact on radionuclide sorption. Van Loon and Glaus (1998) investigated the effect of α- and β-ISA on Eu(III) sorption individually, and found that the α-ISA complex was approximately 100 times more stable than the equivalent β-ISA complex. However, since α-ISA comprises approximately half of the total ISA, the potential variations in the aqueous phase concentration of α-ISA due to the experimental setup and sorption are greater any effect due to the presence of β-ISA. Therefore, the discussion below does not specify whether ISA or α-ISA was used in each experiment. It is also worth noting that different experimental approaches, such as the order in which the ligand and metal are added and the times between these, may affect short term results due to kinetics (e.g. Reinoso-Maset et al. 2012).

The effect of ISA on Eu(III) sorption has been investigated in a number of studies. Van Loon and Glaus (1998) found that ISA concentrations > 1×10^{-4} M affected Eu(III) sorption to feldspar in artificial cement porewater. Dario et al. (2004) found that short term (24 hours) Eu(III) sorption to hydrated cement was reduced when ISA was added at concentrations of 10^{-3} and 10^{-2} M. Changes over 400 days were investigated using $10^{-2.5}$ M ISA and although Eu(III) sorption increased during the first 50 days, ISA reduced the sorption of Eu(III) at equilibrium by over an order of magnitude. Wieland et al. (1998) found that ISA had a negligible effect on Eu(III) sorption to hydrated cement until the ISA concentration exceeded 10^{-2} M. Europium sorption on hardened cement paste was reduced by a factor 100 at equilibrium concentrations of ~ 10^{-1} M ISA (Bradbury and Van Loon 1997).

ISA was found to reduce Th(IV) sorption to hardened cement paste by over four orders of magnitude as the ISA equilibrium concentrations increased from 10^{-4} to 10^{-2} M, but it had no influence at concentrations ≤ 10^{-4} M (Bradbury and Van Loon 1997, Wieland et al. 1998, Wieland and Tits 2002). Van Loon and Glaus (1998) found that ISA concentrations in the range 10^{-4} – 10^{-3} M reduced Th(IV) sorption to feldspar. Experiments by Pavasars (1999) showed that the addition of a high concentration of ISA (3×10^{-2} M) resulted in a persistent reduction of radionuclide sorption; after 3 months Th(IV) sorption was reduced at least 50 times. However, lower concentrations (3×10^{-3} – 5×10^{-3} M ISA) only reduced sorption of ^{234}Th(IV) significantly for 1 month (Pavasars 1999).

More recently, Tasi (2018) examined the effect of ISA on Pu(IV) sorption to cement. In the most relevant experiments for this report, ISA was present at a total concentration of 10 mM, the initial Pu concentration was 4×10^{-9} M and the S:L ratio was 2–4 g/L. Two sets of experiments were carried out. The first set involved equilibrating the hydrated cement phase, Pu and redox buffer in the porewater solution, with subsequent addition of ISA, while the second set involved equilibrating Pu and ISA in the redox-buffered porewater solution, with subsequent addition of fresh cement powder. Sorption of Pu(IV) was reduced by a factor of 1 000 when Pu was pre-equilibrated with the cement, and a factor of 32 000 when Pu was pre-equilibrated with ISA. Tasi (2018) judged that the first set of experiments were most representative of equilibrium conditions.

ISA has also been found to reduce Ni(II) sorption to feldspar, but significant effects were only seen at ISA concentrations higher than 10^{-2} M (Van Loon and Glaus 1998). The degradation products of cellulosic materials (tissues, cotton and paper) were more effective at solubilising Ni(II), but these have not been fully characterised or studied to the same extent as ISA (Van Loon and Glaus 1998, Van Loon et al. 1999b). Recently, Bruno et al. (2018) examined the effect of ISA on Ni(II) sorption to cement and observed a reduction in Ni(II) sorption at an ISA concentration of 4×10^{-3} M, of between 1.2 and 2.4 times. With a 2×10^{-2} M ISA concentration, sorption was reduced by a factor of 3–6.

The sorption of anionic species may also be reduced by the presence of ISA through competition for surface binding sites. Sorption of SeO_3^{2-} to non-degraded (pH 13.3) and degraded (pH 12.0) hardened cement paste was reduced by a factor of two by the addition of 2×10^{-3} and 5×10^{-4} M ISA, respectively (Pointeau et al. 2008).

Impact of PAN filter aid degradation products

Dario et al. (2004) investigated the effect of UP2 degradation products on the sorption of ^{152}Eu to cement, and these data were also presented in Duro et al. (2012). The experiments used an initial UP2 fibre concentration of 25 g L^{-1}, which is broadly similar to the concentration expected in 1–2BTF. The degradation products obtained at pH 12.5 (buffered by $Ca(OH)_2$) and room temperature did not affect Eu sorption significantly. The maximum degradation product concentration in this experiment (approximately 8 mg L^{-1} DOC) was equal to the maximum concentration obtained in the associated degradation experiments, when the on-going rate of degradation was very slow. However, a similar concentration of degradation products obtained at pH 13.4 reduced Eu(III) sorption significantly.

This suggests that the disposal of UP2 in bitumen conditioning is preferable since it will reduce both UP2 degradation (Section 2.2.3) and the complexing power of the degradation products. This is the case for F.17 waste packages that are disposed of in 1–2BMA. However, the greatest concentrations of UP2 are in 1–2BTF, and this waste (O.07) is dewatered and disposed of in concrete tanks. As mentioned earlier, further experiments are being carried out to better understand the long-term degradation of UP2. Therefore, UP2 is not considered further in this report, although it is acknowledged that it is potentially of significant concern in 1–2BTF and the silo.

Impact of gluconate

Gluconate has been seen to form stable complexes with, for example, Ni(II) (Warwick et al. 2003), U(IV) (Warwick et al. 2004), Th(IV) (Colàs 2014), U(IV) (Colàs 2014) and Np(IV) (Rojo et al. 2013) under alkaline conditions. The stability constant derived for the $Np(OH)_4GLU^-_{(aq)}$ complex indicated that gluconate would dominate Np(IV) speciation when the free dissolved gluconate concentration exceeds 10^{-6} M (Rojo et al. 2013). The stability constant was consistent with the linear free energy relationship between analogous Th(IV)-, U(IV)- and Pu(IV)-GLU aqueous complexes (Rojo et al. 2013). The relationship between the stability of $An(IV)(OH)_4GLU^-_{(aq)}$ and $An(IV)(OH)_{4(aq)}$ complexes was constant for the actinides investigated.

The effect of gluconate on radionuclide sorption has been studied to a lesser extent than ISA, and with a particular focus on Eu sorption. Gluconate was found to reduce Eu sorption to hydrated cement by approximately three orders of magnitude at gluconate concentrations above 10^{-4} M (Nordén 1994), however, the Eu concentrations recovered to their original values within approximately 200 days. More recently, Dario et al. (2004) found that 10^{-5} - 10^{-4} M gluconate decreased Eu sorption to hydrated cement by up to 4 orders of magnitude after 24 hours. With $10^{-4.5}$ M gluconate, this was followed by rapid sorption of Eu(III) over the following days resulting in a negligible long-term effect.

Here, as with ISA, sorption of the organic complexing agent makes the results particularly sensitive to the experimental set-up.

Impact of other complexing agents used at the nuclear power plants

The complexing agents used to the greatest extent at Swedish nuclear power plants are citrate, oxalate, NTA (and its derivatives), EDTA and gluconate (Keith-Roach et al. 2014). The ability of these complexing agents to form complexes with radionuclides is affected by the high pH conditions and high Ca^{2+} concentrations of a cementitious repository, due to the stability of radionuclide–hydroxy species and Ca^{2+}–organic complexes. Speciation calculations for Swiss cementitious repository scenarios (pH = 11–13, Ca^{2+} concentration = 0.001–0.1 M) suggested that Ni(II), Mn(II) and Pb(II) would be the only radionuclides to be complexed and that EDTA would be the only complexing agent of significance (Hummel 1993). A reduction in the sorption of Ni(II) and Mn(II) was calculated when the EDTA concentration exceeded 10^{-4} M, and a reduction in the sorption of Pb was calculated when the EDTA concentration exceeded 10^{-3} M. In the absence of experimental data, Bradbury and Van Loon (1997) selected a hydrated cement sorption reduction factor of 50 for Ni(II) and its chemical analogues when the porewater concentration was 4.6×10^{-2} M EDTA. Since Pb(II) forms weaker complexes with EDTA, a sorption reduction factor of 5 was used.

Experimental data have also shown that EDTA can have a temporary effect on radionuclide sorption. For example, sorption of Am(III) to hydrated cement was initially reduced by an EDTA concentration of 1.5×10^{-3} M (Allard and Andersson 1987), but after a period of weeks to months, sorption increased

to a point that the EDTA no longer affected the solution phase Am(III) concentration. Sorption was much slower with 3×10^{-2} M EDTA but, after one year, the Am(III) concentration was the same as in the absence of EDTA.

More recent experiments have shown that EDTA, NTA and citrate reduce Eu(III) sorption to hydrated cement at concentrations $\geq 10^{-3}$ M in the short term (24 hours) (Dario et al. 2004). The variation over 400 days was also investigated using EDTA, NTA and citrate concentrations of 10^{-2} M. Eu(III) sorption increased to reach or approach equilibrium by ~100 days. Long-term Eu(III) sorption was reduced by EDTA (4 orders of magnitude), citrate (1–2 orders of magnitude and, to a lesser extent, NTA (> 0.5 of an order of magnitude).

The modelling in Hummel (1993) described above shows the importance of concurrent and competing reactions and is a useful demonstration of the complexity of radionuclide–ligand interactions. However, there have been improvements in the thermodynamic understanding of radionuclide-complexing agent interactions in the past 25 years. In order to understand the impact of the experimentally observed effects at repository scale, PhreeqC modelling was carried out using the version 9 of the Thermochimie database (Giffaut et al. 2014) (see Appendix 3). First, the solution phase speciation of Am(III) was calculated in the presence of the portlandite concentrations used in Dario et al. (2004), as a particular complexing agent was titrated in. Am(III) was used as an analogue of Eu(III), and the calculated results were generally consistent with the effects on sorption seen in the experiments. The next stage involved increasing the concentration of portlandite to be representative of concentrations in SFR. For trivalent actinides, the calculations demonstrated that while ISA, NTA and citrate affect Am(III) speciation under the experimental conditions of Dario et al. (2004), only ISA was important under conditions with a concentration of portlandite typical for SFR. For NTA, this was due to preferential formation of Ca-NTA complexes. For citrate, only a very small proportion of Am(III) was present as a citrate complex even in the absence of Ca^{2+}, due to the preferential formation of hydroxide species. The presence of Ca^{2+} reduced the proportion of Am(III) present as a citrate complex further. When Th(IV) was included in the calculations, both ISA and NTA were found to control Th(IV) speciation in the presence of the representative concentration of portlandite. Hydrolysed Am(III)-ISA, Th(IV)-ISA and Th(IV)-NTA species are included in the database, which are highly stable at high pH. Citrate was not found to be important for Th(IV) speciation under representative conditions.

Impact of cement additives

Research relating to the impact of cement additives on radionuclide solubility and sorption has focussed on superplasticisers. Different types of superplasticisers have been shown to increase the solubility of radionuclides, including Ni(II), Tc(IV), U(IV), Pu(IV), Am(III) (Keith-Roach and Höglund 2018).

Experiments investigating the impact of superplasticisers on radionuclide sorption have often been carried out by adding superplasticisers and radionuclides to HCP. Examples include studies of Sikament 10, which prevented measurable Pu sorption to grout with a solution phase concentration of 0.5 or 1 % (Boult et al. 1998). A further study showed that Sikament 10 reduces Eu(III) sorption to HCP, with a clear effect seen with Sikament 10 added as 0.01 % of the solution phase (solid:liquid ratio of 1 g/L) (Dario et al. 2004).

Dario et al. (2004) also investigated the effect of six other superplasticisers used by SKB on the sorption of Eu(III) to Portland cement. All of the superplasticisers began to exhibit an effect on Eu(III) sorption when they were added at 0.001–0.01 % of the solution phase. The results showed that the highest degree of Eu(III) sorption reduction occurred with Peramin Conpac 30, a PCE superplasticiser, which reduced Eu sorption by 2.5 orders of magnitude. Conversely, Wieland et al. (2014) found that neither a polycarboxylate ether (PCE) nor a polynaphthalene sulfonate (PNS) superplasticiser had a significant effect on Ni, Eu(III) or Th sorption to HCP. The maximum concentrations of SP added to the solution phase in the Eu experiments were around 0.2 g/L (0.02 %), which was higher than the lowest concentrations that had an effect in Dario et al. (2004).

The data obtained from this type of experiment are difficult to relate to repository conditions due to the large difference in the S:L ratio and because superplasticisers are added to cement during casting, rather than present in the solution phase. The components of the superplasticiser product that remain in solution during cement hydration differ from the original superplasticiser, and comprise unreacted

reagents, monomers and oligomers rather than polymers (Keith-Roach and Höglund 2018). Over time, the superplasticiser compounds that leach from cement, if any, will be degradation products, which may be similar to the initial material in the porewater. However, both are rather different from the superplasticiser polymer that dominates the organic material in the product used.

The NDA (2015) carried out a variety of experiments to examine the effect of superplasticisers on radionuclide immobilisation in cement and the main observations are summarised in Table 2-3. As expected, superplasticisers enhanced radionuclide solubility in cement-equilibrated water. Furthermore, superplasticisers resulted in elevated radionuclide concentrations in cement bleed water when the radionuclides were mixed with the grout as it was cast. This observation is relevant for the use of superplasticisers in cement and concrete waste stabilisation matrices. However, radionuclides were only measurable in cases with a high amount of bleed water. Also, the amount of superplasticiser used in industry is generally optimised with regard to the best effect with as little as possible wastage, i.e. the amount of superplasticiser that does not bind to the cement is minimised. Laboratory experiments may therefore result in higher concentrations of superplasticiser components in the initial porewater than in real industrial applications (Keith-Roach and Höglund 2018). To ensure that this is the case, SKB has introduced acceptance criteria for the use of superplasticisers in waste solidification matrices, and these state that it must be demonstrated that minimal amounts of superplasticiser are released into the bleed water (Hedström 2019).

Despite the effect seen in the bleed water, superplasticisers added during casting did not enhance radionuclide mobilisation or transport once the cement had hardened (see Table 2-3). Glaus et al. (2003) also found that the use of commercially available superplasticisers in the preparation of HCP did not affect the sorption of radionuclides. Furthermore, there was no evidence of degradation of the superplasticisers into products with higher complexing power over ~4 months. The effect of superplasticisers in SFR is therefore expected to be limited.

Table 2-3. Summary of the NDA (2015) superplasticiser (SP) experiments with radionuclides (RN).

Experiment	Procedure	Results
Solubility experiment	SP+ RN added to cement equilibrated water	Effect seen for all SP except one preparation that had been dialysed
Through diffusion experiments	Grout cast with 0.5 % SP and cured, 6-month diffusion experiments using RN in solution phase	No diffusion seen
Intact leaching experiments	Grout cast with 0.5 % SP and RN, cured then leached for a maximum of 36 days	RN present in the bleed water when SP were used (which were thought to carry into the curing water to an extent), but no significant effect in the leach tests
Crushed leaching experiments	Grout cast with 0.5 % SP and RN, cured then crushed. Half of the samples irradiated 1.04 MGy @ 0.85 kGy/h. Leached max 24 h.	RN did not leach significantly with reference to the blank

Impact of complexing agents on radionuclide sorption to bentonite

The effect of complexing agents on radionuclide sorption to and diffusion through bentonite is not well defined, reflecting the lack of relevant experiments and the general complexity of ternary processes.

Speciation of the radionuclide–organic complexes is an important consideration in terms of the available diffusion porosity and the effective diffusion coefficient in bentonite. These parameters are much lower for anions than for cations and neutral species. Speciation also affects sorption to surface binding sites. However, bentonite buffers the pH of the porewater (e.g. Gaucher et al. 2005, Cronstrand 2016), and thus affects speciation, and the measurement of bentonite porewater composition is challenging.

Furthermore, the concentration of complexing agents in bentonite is affected by possible sorption to edge sites in the bentonite, by analogy with Al-oxides (Kummert and Stumm 1980), and this has not been quantified to our knowledge. Very low K_d values were calculated for acetate sorption to bentonite

in Ochs and Talerico (2003), but more complex organics with two carboxyl groups may sorb significantly on clay edge sites (Ochs and Talerico 2004). Overall, the speciation, sorption and the persistence of radionuclide–organic complexes in bentonite is uncertain.

Wold (2003) found that humic substances, which are complex organic colloids, can enhance Eu(III) diffusion though compacted bentonite. The interactions between metals/radionuclides and humic substances are more complex than in a radionuclide–organic complex. While thermodynamics controls sorption onto exchangeable sites, further transfer of the metal into non-exchangeable sites in the humic substance is kinetically controlled (Bryan et al. 2012). Metal release from the non-exchangeable sites is a relatively slow kinetically controlled process, and so humic-bound Eu(III) transport may not be a good analogy for complexes. Despite this, the results indicate that organic molecules are not excluded from the bentonite pore space.

2.3.3 Influence of complexing agents on cement integrity

Many complexing agents form complexes with Ca^{2+}, and this affects the equilibrium between dissolved Ca^{2+} and portlandite. Complexation can therefore theoretically enhance cement degradation (De Windt et al. 2015). Additionally, reactions associated with the degradation of organic compounds often involve alkaline hydrolysis, which consumes hydroxide. Therefore, both Ca^{2+} complexation and degradation reactions can potentially affect the integrity of cement.

Cellulose is a major waste component that degrades via alkaline hydrolysis and can be used to indicate the extent to which alkaline hydrolysis can affect cement integrity in SFR. The overall chemical formula of cellulose is $(C_6H_{10}O_5)_n$, although the reactive end group has the formula $C_6H_{11}O_6R$. Therefore, 1 mole of OH^- is consumed for 100 % degradation of 162 g of the initial cellulose present, or 1 mole of portlandite for 324 g of cellulose.

The effect of ISA will be greatest in the waste types that have the highest cellulose:hydrated cement ratio, which in SFR are type F.23 in steel packaging (mass ratio of 16 kg:214 kg). In each F.23 steel waste package, 50 moles of portlandite are expected to be consumed in the degradation of the 16 kg of cellulose (see above). Assuming 2.96 mol $Ca(OH)_2$ per kg dry cement clinker, and that hydrated cement is 64 % clinker, 405 moles of portlandite are present in each F.23 steel waste package. Therefore, based on OH^- consumption, it is expected that about 11 % of the cement in F.23 steel waste packages would degrade as a result of cellulose degradation. Based on an 80 % ISA yield and 100 % complexation of Ca^{2+} by ISA (which is a slight overestimation considering the results in Appendix 3), ~20 % of the cement would degrade. Although both of these estimates are considerable, the majority of the cement is expected to persist even in this worst-case waste type. The effect will be less marked when larger parts of SFR are considered, due to the additional cement in the other waste packages and the concrete structures.

3 Complexing agents in SFR

This chapter compiles the masses of cellulose and complexing agents in defined parts of SFR (the waste packages, 1BMA compartments, and the waste-containing structures and vaults of 1–2BMA, the silo and 1–2BTF), and converts the data into complexing agent concentrations.

The BLA waste packages and vaults are not considered in this report due to their very low radionuclide inventories (~0.2 % of the total radionuclide inventory in SFR; SKB 2013), and because *good retention* is not a BLA safety function. However, high ISA concentrations in the BLA vaults could be of interest in the future in terms of the potential influence on other repository parts.

3.1 Quantities and volumes

The volume of water that will be present in a given waste package or part of SFR following resaturation needs to be known in order to estimate concentrations of dissolved complexing agents. Here, this volume is assumed to be represented by the pore and void volume of the repository part considered. Most pore and void volumes are available from the Inventory report (SKB 2019) and the Initial state report, for which an internal, provisional, partly reviewed and approved PSAR version exists (SKB 2018). However, the pore volumes of the waste packaging are not included in the Inventory report (SKB 2019). Therefore, the pore volume of the waste packaging material has been converted from the mass of concrete reported in the Inventory report (SKB 2019) using the values given in Table 3-1 for structural concrete (general recipe). Additionally, 0.443 m^3 of concrete conditioning was added to the amount reported in the Inventory report (SKB 2019) for S.23:D waste packages. This reflects a new assessment of the inner volume of double moulds (see the Initial State report (SKB 2018) for details).

Table 3-1. Assumed properties of the cementitious materials in SFR applied in this report. The values are consistent with those derived for the Data report.

	Mass of hydrated cement per mass cementitious material (kg kg^{-1})	Mass of hydrated cement in cementitious material (kg m^{-3})	Porosity (%)	Bulk density (kg m^{-3})
Concrete conditioning in waste packages	0.38	859		
Cement conditioning in waste packages	1.00			
Silo grout and shotcrete	0.27	475	30	1 790
1BTF grout bottom*	0.23	500	20	2 130
Structural concrete (general recipe)	0.22	515	11	2 340
Structural concrete for the existing 1BMA and 1–2BTF	0.18	412	14	2 260
Structural concrete for 2BMA and the additional concrete structure in 1BMA	0.20	470	11	2 390

* Two different grouts are used in BTF but the grout used in the bottom of the vaults comprises around 90 % of the total grout used, and its properties are applied to all BTF grout in this report.

The mass of hydrated cement in each waste package and defined part of SFR is also required to account for sorption of ISA and gluconate. Masses (Inventory report, SKB 2019) or volumes (Initial state report, SKB 2018) of cementitious materials were therefore converted into masses of hydrated cement using the data given in Table 3-1.

The total void and pore volume of each waste package that contains cellulose or complexing agents is given in Table 3-2. For each defined part of SFR (each 1BMA compartment, the waste-containing structure in each vault, and each vault), the pore and void volume given in the Initial state report (SKB 2018) has been applied and the values are given in Table 3-3. For 1–2BTF, the waste-containing structure is defined by the grouted volume including the concrete floor and lid.

Table 3-2. Mass of hydrated cement and cellulose, and the void and pore volume, in the relevant waste packages of 1–2BMA, the silo and 1BTF, including the packaging material (SKB 2019). The presence of complexing agents is also noted, see Table 3-4 for details. ":D" indicates waste from decommissioning "_C" and "_S" denote concrete and steel packaging when both are possible for a given waste type.

Waste type	Hydrated cement (kg)	Void + pore volume (m^3)	Cellulose (kg/package)	Contains complexing agents?
Silo				
B.04	248	0.07		Yes
C.02	1322	0.32		Yes
C.24	685	0.65	14.4	
O.02	1465	0.30	1.0	Yes
R.16	1643	0.39		Yes
R.24	1011	0.25	3.9	
S.11	1312	0.41	2.0	
V.24	645	0.84	1.0	
1-2BMA				
B.23_C	1131	0.33	4.0	
B.23_S	627	0.81	20	
C.23	567	0.79	48	
F.05	0	0.07	0.42	
F.15	2238	0.40	0.39	
F.17*	0	0.34	4.3	Yes
F.23_C	625	0.47	19.4	
F.23_S	214	0.93	16.0	
O.01	1212	0.35	9.2	
O.23	788	0.49	6.7	
R.10	1227	0.35		Yes
R.15	1633	0.39		Yes
R.23_C	1006	0.30	3.9	
R.23_S	627	0.85	18.3	
S.09	180	0.06		Yes
S.23:D	1613	0.60	8.0	
V.23	645	0.84	1.0	
V.23:D_C	995	0.38	0.2	
V.23:D_S	1014	0.46	0.4	
1-2BTF**				
B.07	2211	2.05		Yes
O.07	2211	2.86		Yes
R.23_C	1006	0.30	3.9	

* Cellulose is in 195 of the F.17 waste packages.

** O.01 is disposed of in 1BTF but the variant (O.01:09 20) does not contain cellulose.

Table 3-3. Masses of hydrated cement and pore volumes in defined parts of SFR.

	Hydrated cement (kg)				Pore and void volume (m^3)			
	Waste packages	Structural concrete	Grout and shotcrete	TOTAL	Waste packages	Structural concrete	Empty space, grout, shotcrete	TOTAL
1BMA compartment								
1	7.1×10^{5}	2.1×10^{5}	0	9.2×10^{5}	1.7×10^{2}	5.7×10^{1}	7.6×10^{1}	3.0×10^{2}
2	1.9×10^{5}	1.8×10^{5}	0	3.7×10^{5}	2.0×10^{2}	4.8×10^{1}	2.7×10^{2}	5.2×10^{2}
3	1.9×10^{5}	1.8×10^{5}	0	3.6×10^{5}	1.8×10^{2}	4.8×10^{1}	2.0×10^{2}	4.3×10^{2}
4	6.8×10^{5}	1.8×10^{5}	0	8.6×10^{5}	2.1×10^{2}	4.8×10^{1}	7.6×10^{1}	3.4×10^{2}
5	1.9×10^{5}	1.8×10^{5}	0	3.6×10^{5}	1.6×10^{2}	4.8×10^{1}	2.5×10^{2}	4.6×10^{2}
6	1.9×10^{5}	1.8×10^{5}	0	3.7×10^{5}	1.6×10^{2}	4.8×10^{1}	2.7×10^{2}	4.8×10^{2}
7	6.5×10^{5}	1.8×10^{5}	0	8.3×10^{5}	1.9×10^{2}	4.8×10^{1}	7.6×10^{1}	3.1×10^{2}
8	4.9×10^{5}	1.8×10^{5}	0	6.7×10^{5}	3.0×10^{2}	4.8×10^{1}	7.6×10^{1}	4.2×10^{2}
9	6.1×10^{5}	1.8×10^{5}	0	7.9×10^{5}	2.1×10^{2}	4.8×10^{1}	7.6×10^{1}	3.4×10^{2}
10	3.8×10^{5}	1.8×10^{5}	0	5.6×10^{5}	2.5×10^{2}	4.8×10^{1}	9.3×10^{1}	3.9×10^{2}
11	2.4×10^{5}	1.8×10^{5}	0	4.2×10^{5}	1.8×10^{2}	4.8×10^{1}	5.4×10^{2}	7.7×10^{2}
12	1.5×10^{4}	1.8×10^{5}	0	1.9×10^{5}	1.7×10^{1}	4.8×10^{1}	9.8×10^{2}	1.0×10^{3}
13	0	1.8×10^{5}	0	1.8×10^{5}	1.4×10^{1}	4.8×10^{1}	1.0×10^{3}	1.1×10^{3}
14	0	7.6×10^{4}	0	7.6×10^{4}	2.9×10^{1}	2.2×10^{1}	1.1×10^{2}	1.6×10^{2}
15	0	7.6×10^{4}	0	7.6×10^{4}	2.6×10^{1}	2.2×10^{1}	1.3×10^{2}	1.7×10^{2}
Total 1BMA structure	4.5×10^{6}	2.5×10^{6}	0	7.0×10^{6}	2.3×10^{3}	6.8×10^{2}	4.2×10^{3}	7.2×10^{3}
1BMA vault	4.5×10^{6}	2.5×10^{6}	1.9×10^{5}	7.2×10^{6}	2.3×10^{3}	6.9×10^{2}	1.5×10^{4}	1.8×10^{4}
2BMA								
2BMA caissons	7.3×10^{6}	7.4×10^{6}	0	1.5×10^{7}	3.8×10^{3}	1.7×10^{3}	8.3×10^{3}	1.4×10^{4}
2BMA vault	7.3×10^{6}	8.7×10^{6}	2.3×10^{6}	1.8×10^{7}	3.8×10^{3}	2.0×10^{3}	3.5×10^{4}	4.0×10^{4}
Silo								
Silo structure	1.1×10^{7}	5.2×10^{6}	2.9×10^{6}	2.0×10^{7}	3.3×10^{3}	1.1×10^{3}	1.8×10^{3}	6.3×10^{3}
Silo vault	1.1×10^{7}	5.2×10^{6}	2.9×10^{6}	2.0×10^{7}	3.3×10^{3}	1.1×10^{3}	7.2×10^{3}	1.2×10^{4}
1–2BTF								
1BTF waste block	1.6×10^{6}	8.2×10^{5}	2.1×10^{6}	4.5×10^{6}	1.3×10^{3}	2.8×10^{2}	8.3×10^{2}	2.4×10^{3}
1BTF vault	1.6×10^{6}	8.7×10^{5}	2.2×10^{6}	4.6×10^{6}	1.3×10^{3}	2.9×10^{2}	5.2×10^{3}	6.8×10^{3}
2BTF waste block	1.7×10^{6}	8.2×10^{5}	8.8×10^{5}	3.4×10^{6}	1.9×10^{3}	2.8×10^{2}	3.5×10^{2}	2.5×10^{3}
2BTF vault	1.7×10^{6}	8.7×10^{5}	1.0×10^{6}	3.6×10^{6}	1.9×10^{3}	2.9×10^{2}	4.7×10^{3}	6.9×10^{3}

The mass of cellulose in each waste type has been evaluated in the most recent assessment of the waste inventory (SKB 2019). This new assessment has reduced the mass of cellulose reported previously for several waste packages (Table 3-2). The inventory report (SKB 2019) does not report the 4.3 kg of cellulose estimated to be present in 195 of the F.17 waste packages, but this is taken into account here.

The mass of complexing agents present in SFR was derived in Appendix 2 and the masses per waste package are given in Table 3-4. The majority of complexing agents that will be disposed of in SFR come from pre-2012 activities because of the introduction of more stringent waste acceptance criteria in 2012[4]. The complexing agents identified comprise citrate, gluconate, EDTA, NTA, methylglycine diacetate (MGDA), oxalate and sodium capryliminodipropionate (NKP). Since MGDA is structurally very similar to NTA, see Figure 3-1, it has been included as NTA in this report. The complexing agents in some waste packages have been assessed in a number of different time periods and so Table 3-4 shows the maximum of these.

[4] **Almkvist L, 2012.** Acceptanskriterier för avfall i SFR. SKBdoc 1336074 ver 1.0, Svensk Kärnbränslehantering AB. (In Swedish.) (Internal document.)

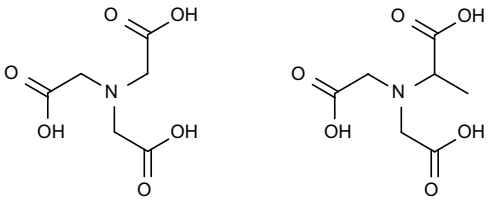

Figure 3-1. *Chemical structures of NTA and MGDA.*

Table 3-4. Mass of complexing agents per waste package in SFR. Note that S.09, O.07 and B.07 show the maximum concentration of each complexing agent identified in different assessments. EDTA is only present in waste packages from Barsebäck, Forsmark, Oskarhamn and Ringhals that were produced up to the end of 1998, and from SVAFO/Studsvik Nuclear up to the end of 2006.

Waste type	Type of packaging	Number of waste packages that contain complexing agents	EDTA (kg/package)	NKP[a] (kg/package)	NTA (kg/package)	Citrate (kg/package)	Oxalate (kg/package)	Sodium gluconate (kg/package)
1BMA								
F.17	Steel	608[b]	7.1×10^{-3}		8.5×10^{-1}[c]	3.7×10^{-1}	2.1×10^{-2}	3.8×10^{-2}
R.10	Concrete	84	2.8×10^{-3}		8.6×10^{-1}			8.7×10^{-2}
R.15	Steel with concrete lid	147	2.8×10^{-3}		8.6×10^{-1}			8.7×10^{-2}
2BMA								
S.09		715	9.0×10^{-3}		9.0×10^{-3}			3.0×10^{-3}
Silo								
B.04	Steel	349					1.1×10^{-1}	
C.02	Concrete	416			6.8×10^{-2}			
O.02	Concrete	346					1.4×10^{-1}	
R.16	Steel with concrete lid	1445[d]	2.8×10^{-3}		8.6×10^{-1}			8.7×10^{-2}
1−2BTF								
B.07	Concrete	223	1.2×10^{-2}		3.5×10^{-4}	2.5×10^{-1}		3.1×10^{-1}
O.07	Concrete	378	6.6×10^{-3}	5.2	4.0×10^{1}	4.0×10^{1}		

[a] Sodium dicapryliminodipropionate (Fanger et al. 2001).

[b] 352 of these contain EDTA.

[c] Includes MGDA, which has a very similar structure to NTA.

[d] 664 of these contain EDTA.

Table 3-5 shows the distribution of F.17, R.10 and R.15 waste packages that contain complexing agents, and F.17 waste packages that contain cellulose, between the 1BMA compartments.

Table 3-6 summarises the mass of cellulose and complexing agents in each defined part of SFR considered. The mass of cellulose in each vault was taken from the Inventory report (SKB 2019). However, the mass of cellulose in the F.17 waste packages was added, as cellulose was not included in any of these waste packages in the Inventory report (SKB 2019). The mass of cellulose in each 1BMA compartment was obtained directly from SKB and is consistent with the Inventory report (SKB 2019). Therefore, cellulose in the F.17 waste packages was also added to this, according to the distribution shown in Table 3-5. The data provided by SKB are average values from 10 000 Monte Carlo simulations of the content of the waste, based on the Inventory report (SKB 2019). In the silo, 5.2 t of cellulose is estimated to be present in the form of the Methocel cement additive, and this has been added to the amount of cellulose present in the silo. The mass of cellulose in the vaults of interest is considerably lower than estimated previously due to the changes in the amounts per waste package.

Table 3-5. Distribution of 1BMA waste packages that contain complexing agents.

1BMA compartment	F.17	F.17 cellulose*	R.10	R.15
1				
2				
3	144	144		
4				124
5	28	8		
6	259	43		
7				
8			36	
9			48	
10	116			
11	7			23
12	37			
13				
14	14			
15	3			
Total	608	195	84	147

* These waste packages also contain complexing agents.

Table 3-6. Mass (kg) of cellulose (from SKB 2019) and complexing agents (calculated in this report) in the 1BMA compartments, 1BMA, 2BMA, the silo and 1−2BTF.

	Cellulose	Sodium gluconate	EDTA	NKP	NTA	Citrate	Oxalate
1BMA compartment							
1							
2	727						
3	619	5.4			122	53	3.0
4	3180	11	0.3		107		
5	34.4	1.1			24	10	0.6
6	186	9.8	1.3		220	95	5.3
7	1950						
8	4180	3.1	0.1		31		
9	4560	4.2	0.1		41		
10	3470	4.4	0.8		98	42	2.4
11	3730	2.3	0.1		26	2.6	0.1
12	8.1	1.4	0.2		31	14	0.8
13					0		
14		0.5	0.1		12	5.1	0.3
15		0.1	0.02		2.5	1.1	0.1
Total 1BMA	22700	43	3.1		715	222	13
Total 2BMA	9190	0.17	5.2		5.9		
Total silo	11700*	126	1.9		1271		90
Total 1BTF	91		0.5	52	78	86	
Total 2BTF		0.59	4.5	15	3320	3370	

* Includes 5200 kg of Methocel cement additive.

3.2 Uncertainties in the masses of complexing agents and cellulose

The uncertainties associated with the masses of cellulose and complexing agents in each defined part of SFR were assessed in different ways.

The maximum mass of cellulose in the waste in each SFR vault was taken to be the 95th percentile of the 10 000 Monte-Carlo simulations of the waste in the vault. These values are fairly close to the best estimate values (Table 3-7). The minimum was taken to be half the expected mass of cellulose. The minimum was selected to take account of the fact that a significant proportion of the material classified as cellulose, such as cloth, may actually be made of other materials, such as man-made fibres, and that the mass given for a typical waste package is conservative.

Table 3-7. Uncertainties in the mass of cellulose present. Note that the silo also includes 5 200 kg cellulose in a cement additive.

	Best estimate (t)	Maximum (t)	Minimum (t)
1BMA compartment			
1	0	0	0
2	7.3×10^{2}	7.3×10^{2}	3.6×10^{2}
3	6.2×10^{2}	6.2×10^{2}	3.1×10^{2}
4	3.2×10^{3}	3.3×10^{3}	1.6×10^{3}
5	3.4×10^{1}	3.4×10^{1}	1.7×10^{1}
6	1.9×10^{2}	1.9×10^{2}	9.3×10^{1}
7	2.0×10^{3}	2.1×10^{3}	9.8×10^{2}
8	4.2×10^{3}	4.5×10^{3}	2.1×10^{3}
9	4.6×10^{3}	4.8×10^{3}	2.3×10^{3}
10	3.5×10^{3}	4.0×10^{3}	1.7×10^{3}
11	3.7×10^{3}	6.2×10^{3}	1.9×10^{3}
12	8.1×10^{0}	1.0×10^{1}	4.1×10^{0}
13	0	0	0
14	0	0	0
15	0	0	0
Silo	1.2×10^{4}	1.3×10^{4}	5.9×10^{3}
1BMA	2.3×10^{4}	2.6×10^{4}	1.1×10^{4}
2BMA	9.2×10^{3}	9.9×10^{3}	4.6×10^{3}
BRT	0	0	0
1BTF	9.1×10^{1}	9.6×10^{1}	4.5×10^{1}
2BTF	0	0	0

The main uncertainty associated with the estimated masses of complexing agents in the waste is that the information often reflects usage over a relatively short period of time, and this is extrapolated. There are two different approaches that can be used to extrapolate the total masses disposed of:

1. Dividing the mass of a complexing agent used in one year by the number of waste packages produced that year and multiplying by the total number of waste packages produced.
2. Multiplying the consumption in one year by the number of years that the product was used and dividing this amount by the total number of waste packages produced.

Neither approach is perfect since waste package production is not uniform, and the use of detergents and chemicals may also vary over time. The uncertainties associated with extrapolated data (B.07, C.02 and O.07) are evaluated in Table 3-8 by comparing the number of packages produced in the relevant year as a proportion of the total number of packages produced with the reciprocal of the number of years the complexing agent was used. Table 3-1 shows that the highest uncertainty was obtained for citrate in B.07 waste packages. Citrate was not included in the latest estimation from Barsebäck, so the data is extrapolated from Fanger et al. (2001). The uncertainties are lower for C.02 and O.07.

Table 3-8. Comparison of the number of packages produced in the relevant year as a proportion of the total number of packages produced (used in approach 1; actual numbers given in brackets) with the reciprocal of the number of years the complexing agent was used (used in approach 2).

Waste package	Proportion of packages produced (approach 1)	1/number of years (approach 2)	Higher value/lower value (% difference)
B.07 (citrate content only)	0.071 (15/212)	0.036	100
C.02	0.036 (15/416)	0.037	2.8
O.07	0.030 (12/400)	0.040	33

The uncertainties in the mass of NTA is of importance for the sorption reduction factors calculated in Chapter 4, and this is affected by different waste producers in different waste compartment and vaults (F.17, R.10, R.15, R.16 and O.07 contribute significantly to the NTA in different waste compartments and vaults). For simplicity, the maximum mass is assumed to be twice the reference value and the minimum half the reference value in all cases. This encompasses the uncertainties presented in Table 3-2.

The major uncertainty relating to the disposal of PAN type filter aids in SFR, particularly in the BTF vaults due to waste type O.07 and the silo due to waste type C.02, is not included in these uncertainties.

3.3 Concentration calculations

In this section, the concentrations of complexing agents are given within the porewater of each waste type and defined repository parts. The calculations assume 100 % release of the complexing agents from the waste matrix into the porewater. However, the concentrations of gluconate were also calculated following sorption to the available hydrated cement, using Equation (2-4). In the case of ISA, the porewater concentration was calculated from the mass of cellulose present and the extent of cellulose degradation as a function of time (Equation (2-2)), using the parameters for Tela tissue in Glaus and Van Loon (2008). The porewater ISA concentrations were first calculated assuming all ISA is in solution, based on the molecular mass of the cellulose chain that is "peeled off" in every step (162 g/mol, see Equation 2-1). The ISA concentration was also calculated following sorption of ISA to available hydrated cement (Equation (2-4)) and the parameters defined in Van Loon et al. (1997). This is a slightly conservative choice given the greater sorption of ISA to cement determined by Tasi (2018) at pH ~ 12.5.

3.3.1 Concentrations of ISA

Using the cellulose degradation constants derived for Tela tissues, the model of Glaus and Van Loon (2008) predicts that 4, 11, 38, 60 and 99 % of the cellulose in highly alkaline parts of SFR will have degraded after 10, 100, 500, 1 000 and 5 000 years, respectively (see Section 2.2.1). Since ISA comprises ~ 80 % by mass of the cellulose degradation products (Bradbury and Van Loon 1997, Van Loon and Glaus 1997, Van Loon and Glaus 1998, Pavasars et al. 2003, Glaus and Van Loon 2008), the mass of ISA produced after the respective time periods was calculated as 3.2, 9.0, 30, 48 and 79 % of the cellulose present inside each waste package. The assumption that ISA does not migrate out from each vault over time appears conservative, especially at the longer time intervals considered. However, a modelling study suggested that 90 % of the ISA produced in 1BMA will be retained over a 20 000-year period, due to sorption (von Schenck and Källström 2013). Degradation of ISA has not been accounted for, due to the lack of evidence that degradation occurs under alkaline, anaerobic conditions (Section 2.3.1).

The sorption calculations applied the non-linear two site sorption isotherm described in Section 2.3.1 (Equation (2-4)). All of the ISA was included in the sorption calculations, as α- and β-ISA have comparable sorption isotherms (Van Loon and Glaus 1998).

There is evidence that Eu(III) forms more stable complexes with α-ISA than β-ISA (Van Loon and Glaus 1998), which suggests that the α-ISA concentration should be reported. However, the total ISA concentrations are reported here for the following reasons:

- ISA is not often separated into its diastereoisomers for radionuclide sorption experiments.
- α-ISA is expected to precipitate at concentrations above 2×10^{-2} under portlandite-controlled conditions and, when this happens, the ratio of α-ISA: β-ISA will vary between the precipitated, solution and sorbed phases. There has been no experimental investigation of this.
- Sorption of ISA to cement means that the impact of ISA on radionuclide sorption is highly sensitive to the experimental design.
- The data suggesting that β-ISA is a weaker complexing agent than α-ISA is relatively limited, and the stability constant for the Eu β-ISA complex in Van Loon and Glaus (1998) was still reasonably high.

However, where appropriate, the solubility limit for α-ISA is referred to in the results tables to highlight that further increases above this concentration are not likely to equate to a linear increase in complexing power. Note that since the tables show the total concentration of ISA, and α-ISA comprises approximately half of this, the solubility limit for α-ISA is considered to have been reached when the total ISA concentration is twice this limit.

Table 3-9 shows the concentrations of ISA after 5 000 years of cellulose degradation, in the pore and void volume of the waste packages, including the packaging. The concentrations of ISA following sorption to the available hydrated cement are most relevant. Sorption of ISA to hydrated cement reduces the ISA concentration effectively in many of the BMA and silo waste packages. However, in some waste packages, the predicted concentration of ISA exceeds the amount that can be removed effectively by the available hydrated cement present. Therefore, sorption only reduces the solution phase concentrations in these waste packages to a relatively small degree. In some cases, the ISA concentration exceeds the solubility limit for Caα-ISA_2 and precipitation is expected. This could reduce radionuclide mobility within these waste packages according to Chen et al. (2019).

Table 3-9. Concentrations of ISA calculated after 5 000 years of cellulose degradation in the relevant BMA, silo and BTF waste packages, including the concrete packaging material. The ISA concentrations were calculated with and without consideration of sorption to available hydrated cement. When the calculated ISA concentration following sorption was more than twice the expected solubility limit for α-ISA during the portlandite stage of cement degradation (2×10^{-2} M), i.e. 4×10^{-2} M, the solubility limit is given followed by the calculated concentration in brackets.

	ISA concentration – no sorption (M)	ISA concentration following sorption (M)
Silo		
C.24	1.1×10^{-1}	4.7×10^{-3}
O.02	1.7×10^{-2}	2.0×10^{-5}
R.24	7.6×10^{-2}	1.3×10^{-4}
S.11	2.4×10^{-2}	4.6×10^{-5}
V.24	5.8×10^{-3}	4.6×10^{-5}
1-2BMA		
B.23_C	5.9×10^{-2}	1.2×10^{-4}
B.23_S	1.2×10^{-1}	2.0×10^{-2}
C.23	3.0×10^{-1}	4×10^{-2} (1.5×10^{-1})
F.05	3.2×10^{-2}	3.2×10^{-2}
F.15	4.8×10^{-3}	4.9×10^{-6}
F.17*	6.3×10^{-2}	4×10^{-2} (6.3×10^{-2})
F.23_C	2.0×10^{-1}	2.3×10^{-2}
F.23_S	8.4×10^{-2}	4×10^{-2} (4.7×10^{-2})
O.01	1.3×10^{-1}	3.3×10^{-4}
O.23	6.7×10^{-2}	4.0×10^{-4}
R.23_C	6.2×10^{-2}	1.3×10^{-4}
R.23_S	1.1×10^{-1}	1.5×10^{-2}

Table 3-9. Continued.

	ISA concentration – no sorption (M)	ISA concentration following sorption (M)
1-2BMA		
S.23:D	6.5×10^{-2}	1.8×10^{-4}
V.23	5.8×10^{-3}	4.6×10^{-5}
V.23:D_C	2.7×10^{-3}	5.9×10^{-6}
V.23:D_S	3.8×10^{-3}	9.9×10^{-6}
1BTF		
O.01	1.3×10^{-1}	3.3×10^{-4}
R.23_C	6.2×10^{-2}	1.3×10^{-4}

* 195 of the F.17 disposed contain cellulose.

Table 3-10 shows the concentrations of ISA calculated for larger parts of SFR. The ISA concentrations remain well below the expected solubility limit for Caα-ISA_2 in all of these defined parts of SFR considered when sorption is taken into account. The temporal evolution of the ISA concentrations in the1BMA compartments and 1BMA structure are shown in Figure 3-2 and the data are given in Appendix 4.

Table 3-10. Concentrations of ISA calculated in the 1BMA compartments, construction and vault, the 2BMA caissons, the silo construction and vault, and the 1BTF waste zone and vault, after 5 000 years of cellulose degradation, based on the predicted waste distribution at closure. The ISA concentrations were calculated with and without consideration of sorption to available hydrated cement. After sorption, none of the calculated ISA concentrations were above the expected solubility limit for α-ISA during the portlandite stage of cement degradation (2×10^{-2} M).

	ISA concentration (M)	
	No sorption	Sorption
1BMA compartment		
1	0	0
2	6.8×10^{-3}	6.0×10^{-5}
3	7.0×10^{-3}	5.1×10^{-5}
4	4.6×10^{-2}	1.2×10^{-4}
5	3.7×10^{-4}	2.6×10^{-6}
6	1.9×10^{-3}	1.4×10^{-5}
7	3.1×10^{-2}	7.4×10^{-5}
8	4.8×10^{-2}	2.5×10^{-4}
9	6.6×10^{-2}	2.2×10^{-4}
10	4.3×10^{-2}	2.4×10^{-4}
11	2.4×10^{-2}	4.2×10^{-4}
12	3.8×10^{-5}	1.1×10^{-6}
13	0	0
14	0	0
15	0	0
Total 1BMA structure	1.5×10^{-2}	1.1×10^{-4}
1BMA vault	6.2×10^{-3}	1.0×10^{-4}
2BMA caissons	3.2×10^{-3}	1.8×10^{-5}
2BMA vault	1.1×10^{-3}	1.4×10^{-5}
Silo structure	9.2×10^{-3}	1.7×10^{-5}
Silo vault	4.9×10^{-3}	1.7×10^{-5}
1BTF waste block	1.9×10^{-4}	5.7×10^{-7}
1BTF vault	6.5×10^{-5}	5.4×10^{-7}
2BTF waste block	0	0
2BTF vault	0	0

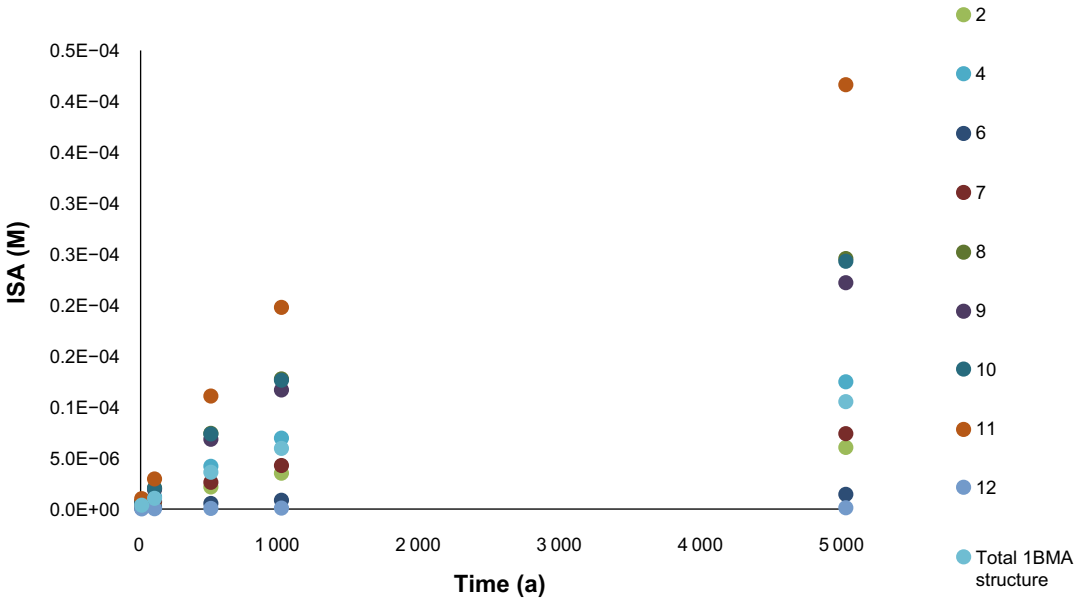

Figure 3-2. *The evolution of the dissolved ISA concentration in the 1BMA compartments (shown by number) from the time of closure, and 1BMA structure accounting for sorption to hydrated cement. The x-axis shows time after closure.*

3.3.2 Concentrations of gluconate

Gluconate undergoes sorption to hydrated cement (see Section 2.3.1), following the non-linear two site Langmuir isotherm (Equation (2-4)) and the sorption constants reported in Glaus et al. (2006; also see Section 2.3.1). The concentrations of gluconate inside the BMA, silo and BTF waste packages (not including the packaging), with and without sorption to the waste conditioning, are presented in Table 3-11. The maximum gluconate concentration in 1 package of a sub-class of the B.07 waste type, B.07:1, is shown in Table 3-11. This sub-class is the only part of B.07 waste to contain gluconate and comprises 11 or 12 packages in total.

Table 3-11. Concentrations of gluconate (M) inside the relevant 1BMA, silo and 1–2BTF waste packages and in the packages including the packaging material. The concentrations were calculated with and without consideration of sorption to hydrated cement.

	No sorption	Sorption
1BMA		
F.17	5.2×10^{-4}	5.2×10^{-4}
R.10	1.1×10^{-3}	4.0×10^{-9}
R.15	1.0×10^{-3}	3.0×10^{-9}
2BMA		
S.09*	2.1×10^{-4}	9.4×10^{-10}
Silo		
R.16	1.0×10^{-3}	3.0×10^{-9}
1–2BTF		
B.07**	6.9×10^{-4}	8.0×10^{-9}

*Gluconate is only present in 56 S.09 waste packages
** Shows the maximum gluconate concentration anticipated inside one waste package from 2011.

Table 3-11 shows that inside every gluconate-containing waste package except F.17, sorption to the available cement reduces the gluconate concentrations effectively. These waste types do not contain cellulose, which avoids the need to assess whether gluconate and ISA compete for surface binding sites.

The bitumen-conditioned F.17 wastes destined for 1BMA are packaged in steel, thus there is no hydrated cement in the waste package for gluconate to sorb to. However, calculations of the gluconate concentrations within the different 1BMA compartments show that dilution and sorption to the hydrated cement lowers the concentration to $\leq 1.5 \times 10^{-9}$ M in every compartment (Table 3-12). The gluconate concentrations in 2BMA, the silo and 1–2BTF are very low, especially once sorption has been taken into account.

Table 3-12. Concentrations of gluconate inside the relevant 1BMA compartments, the silo and 2BTF. The concentrations were calculated with and without consideration of sorption to hydrated cement.

	Gluconate Concentration (M)	
	No sorption	**Sorption**
1BMA compartment		
1		
2		
3	5.8×10^{-5}	8.4×10^{-10}
4	1.5×10^{-4}	7.0×10^{-10}
5	1.1×10^{-5}	1.6×10^{-10}
6	9.4×10^{-5}	1.5×10^{-9}
7	0	0
8	3.4×10^{-5}	2.6×10^{-10}
9	5.7×10^{-5}	3.0×10^{-10}
10	5.1×10^{-5}	4.4×10^{-10}
11	1.4×10^{-5}	3.0×10^{-10}
12	6.2×10^{-6}	4.1×10^{-10}
13	0	0
14	1.5×10^{-5}	3.9×10^{-10}
15	3.0×10^{-6}	8.4×10^{-11}
2BMA		
Caisson	5.6×10^{-8}	6.4×10^{-13}
Vault	1.9×10^{-8}	5.1×10^{-13}
Silo		
Silo construction	9.2×10^{-5}	3.6×10^{-10}
Entire silo	5.0×10^{-5}	3.6×10^{-10}
2BTF		
2BTF waste block	1.1×10^{-6}	9.6×10^{-12}
2BTF vault	3.9×10^{-7}	9.1×10^{-12}

3.3.3 Concentrations of other complexing agents

The aqueous concentrations of all other complexing agents were calculated using the assumption that they remain in solution, with no sorption to hydrated cement. This approach is cautious, but necessary due to the lack of sorption isotherm data or relevant degradation studies in the literature. Precipitation is taken into account using the expected solubility limits. Table 3-13 shows that NTA is the complexing agent with the highest concentrations in the waste packages.

Table 3-13. Concentrations of other complexing agents in the different waste packages of 1BMA, the silo and 1–2BTF, including the concrete packaging. When the calculated citrate and oxalate concentrations are higher than the solubility limit expected under repository conditions, 1.3×10^{-3} M and 1×10^{-5} M, respectively, the maximum is given followed by the calculated concentration in brackets.

	Complexing agent concentration (M)				
	EDTA	**NKP**	**NTA**	**Citrate**	**Oxalate**
1–2BMA					
F.17	7.2×10^{-5}		1.3×10^{-2}	1.3×10^{-3} (5.7×10^{-3})*	1×10^{-5} (6.8×10^{-4})
R.10	2.7×10^{-5}		1.3×10^{-2}		
R.15	2.4×10^{-5}		1.2×10^{-2}		
S.09	4.8×10^{-4}		7.3×10^{-4}		
Silo					
B.04					1×10^{-5} (1.8×10^{-2})
C.02			1.1×10^{-3}		
O.02					1×10^{-5} (5.3×10^{-3})
R.16	2.5×10^{-5}		1.2×10^{-2}		
1–2BTF					
B.07**	2.0×10^{-5}		8.9×10^{-7}	6.4×10^{-4}	
O.07**	7.9×10^{-6}	6.1×10^{-3}	7.3×10^{-2}	1.3×10^{-3} (7.3×10^{-2})	

* Assumes the water that becomes available for citrate dissolution in this bitumen-stabilised waste package is equilibrated with cement.
** Note that O.07 and B.07 show the maximum concentration of each complexing agent from the mass identified in either 1998 or the recent assessment.

The concentrations of EDTA, NKP, NTA, citrate and oxalate were calculated within each compartment of 1BMA, the entire silo and 1–2BTF (Table 3-14). Since significant quantities of complexing agents are only present in waste packages produced up to a certain date, not all packages of a given waste package type will contain complexing agents. For 1BMA, the waste packages that contain complexing agents have been distributed into the compartments as shown in Table 3-5. The distribution of waste packages containing complexing agents between 1–2BTF is shown in Table A2-8[5].

[5] **Hedström S, Bultmark F, Sihm Kvenangen K, 2019.** Konsekvensutredning – Komplexbildare i avfallstyper O.07 och F.17 och deras påverkan på säkerhet efter förslutning. SKBdoc 1877287 ver 3.0, Svensk Kärnbränslehantering AB. (In Swedish.) (Internal document.)

Table 3-14. Concentrations of other complexing agents in each relevant 1BMA compartment and in the silo and BTF. When the calculated oxalate concentration is higher than the solubility limit expected under repository conditions, 1×10^{-5} M, this maximum is given followed by the calculated concentration in brackets.

	Complexing agent concentration (M)				
	EDTA	**NKP**	**NTA**	**Citrate**	**Oxalate**
1BMA Compartment					
1	0	0	0	0	
2	0	0	0	0	
3	0	0	1.5×10^{-3}	6.4×10^{-4}	1×10^{-5} (7.7×10^{-5})
4	3.5×10^{-6}	0	1.7×10^{-3}	0	
5	0	0	2.7×10^{-4}	1.2×10^{-4}	1×10^{-5} (1.4×10^{-5})
6	9.5×10^{-6}	0	2.4×10^{-3}	1.0×10^{-3}	1×10^{-5} (1.2×10^{-4})
7	0	0	0	0	
8	8.1×10^{-7}	0	3.8×10^{-4}	0	
9	1.4×10^{-6}	0	6.4×10^{-4}	0	
10	6.6×10^{-6}	0	1.3×10^{-3}	5.6×10^{-4}	1×10^{-5} (6.7×10^{-5})
11	4.9×10^{-7}	0	1.7×10^{-4}	1.7×10^{-5}	2.1×10^{-6}
12	8.0×10^{-7}	0	1.6×10^{-4}	6.7×10^{-5}	8.1×10^{-6}
13	0	0	0	0	
14	1.9×10^{-6}	0	3.8×10^{-4}	1.6×10^{-4}	1×10^{-5} (2.0×10^{-5})
15	3.8×10^{-7}	0	7.6×10^{-5}	3.3×10^{-5}	3.9×10^{-6}
1BMA structure	1.5×10^{-6}	0	5.2×10^{-4}	1.6×10^{-4}	1×10^{-5} (1.9×10^{-5})
1BMA vault	6.1×10^{-7}	0	2.1×10^{-4}	6.5×10^{-5}	7.8×10^{-6}
2BMA					
2BMA structure	1.3×10^{-6}	0	2.2×10^{-6}	0	
2BMA vault	4.4×10^{-7}	0	7.7×10^{-7}	0	
Silo					
Silo structure	1.0×10^{-6}	0	1.1×10^{-3}	0	1×10^{-5} (1.6×10^{-4})
Entire vault	5.5×10^{-7}	0	5.7×10^{-4}	0	1×10^{-5} (8.6×10^{-5})
1BTF					
1BTF waste block	7.6×10^{-7}	7.4×10^{-5}	1.7×10^{-4}	1.9×10^{-4}	0
1BTF vault	2.7×10^{-7}	2.6×10^{-5}	6.0×10^{-5}	6.6×10^{-5}	0
2BTF					
2BTF waste block	6.1×10^{-6}	2.1×10^{-5}	6.9×10^{-3}	7.0×10^{-3}	0
2BTF vault	2.2×10^{-6}	7.6×10^{-6}	2.5×10^{-3}	2.5×10^{-3}	0

4 Sorption reduction factors

Radionuclide transport is affected by the sorption of radionuclides, and sorption to cement is particularly important in SFR. Since complexing agents may reduce the sorption of radionuclides to cement, sorption reduction factors (SRF) are used in the radionuclide transport calculations to reduce the K_d values applied accordingly. Radionuclides in specific oxidation states are grouped according to their chemical properties and SRF are assigned to each group. In SR-PSU, the complexing agent with the highest concentration in a given 1BMA compartment, 2BMA caisson or vault was used to determine the SRF. For each group of radionuclides, a "no-effect" concentration was identified, under which the complexing agents were assumed to have no effect on sorption. An SRF was also identified which, for most radionuclides, increased in a stepwise fashion with every 10-fold increase in the complexing agent concentration (SKB 2014a**)**.

The following changes to the approach were implemented for SR-PSU (PSAR):

- At the compartment, structure or vault level, ISA, NTA, citrate and NKP concentrations were calculated to exceed 2×10^{-5} M, the lowest no-effect concentration identified in Table 4-1 and in the F-PSAR Data report (Tables 7-11a–c in SKB 2014a). However, the NKP concentration is always lower than the NTA concentration and the calculations in Appendix 3 suggest that citrate will not complex radionuclides under the conditions of SFR. Therefore, SRF were calculated based on ISA and NTA concentrations only.
- The relationship between the ISA and NTA concentrations and radionuclide sorption reduction were assessed separately.
- SRF were calculated using a linear relationship with complexing agent concentration rather than a stepwise increase for all species except Pb(II) and Pd(II)[6].
- In each defined part of SFR considered and for each group of similar radionuclides, SRF were calculated with both ISA and NTA, then the maximum SRF was identified and applied. Strictly, the SRF should be added together, but this was judged to be unnecessary in light of the uncertainties involved in the individual SRF.
- Since NTA is not considered to sorb to the cement, its concentrations will decrease over time, as defined by a non-sorbing tracer in the radionuclide transport model. Therefore, when NTA initially resulted in the higher SRF, a second SRF (SRF2) was defined for any long-term impact from ISA, together with a time when the NTA concentration is too low to have an effect. The ISA concentration was considered to be reasonably constant because of its high affinity for cement phases.
- The decrease in the NTA concentration was accounted for in the radionuclide transport model by decreasing the SRF linearly over the time from closure to the implementation of SRF2.
- The uncertainties given in Section 3.2 were used to calculate maximum and minimum SRF, and these are applied in the probabilistic radionuclide transport calculations

[6] For Pb(II) and Pd(II), a single SRF of 100 is applied to all ISA concentrations that exceed the no-effect concentration. This is the same approach as in SR-PSU (Section 7.9 in SKB 2014a).

The ISA and NTA concentrations are presented in Chapter 3. Table 4-1 shows the equations used here to describe the relationships between the concentrations and the SRF values. The table furthermore shows the no-effect concentrations below which no effect of the complexing is seen (SRF = 1). The equations apply ISA and NTA concentrations in units of mM. Since NTA was judged to have no effect on the sorption of trivalent and hexavalent actinides or Pb(II) and Pd(II) in the presence of a cement concentration representative of SFR, the SRF for these radionuclides is always defined by ISA.

Table 4-1. No-effect concentration and equation(s) used to define the SRF for ISA and NTA as a function of [ISA] (mM).

Radionuclides	ISA		NTA	
	No-effect concentration (mM)	SRF	No-effect concentration (mM)	SRF
Ac(III); Eu(III), Am(III), Cm(III), Ho(III), Pu(III),Sm(III), Se(IV), Po(IV), Np(V), Pu(V)	0.1	10 × [ISA]	N/A	1
Pb(II), Pd(II)	0.02	100	N/A	1
Th(IV), Np(IV), U(IV), Pa(IV), Tc(IV), Zr(IV), Sn(IV), Nb(V), Pa(V)	0.1	0.1−1 mM: 110 × [ISA] − 10 1−10 mM: 1 100 × [ISA] − 1 000	0.1	0.1−1 mM: 110 × [NTA] – 10 1−10 mM: 1 100 × [NTA] − 1 000
Pu(IV)	0.1	100.9 × [ISA] − 9	0.1	100.9 × [NTA] − 9
U(VI), Pu(VI)	0.5	2 × [ISA]	N/A	1

Table 4-2 shows the SRF calculated for the initial period (SRF1), while Table 4-3 shows the SRF (SRF2) calculated for when the NTA concentration has dropped below the no-effect level and the time from which the SRF2 values are applied. Both tables give reference SRF as well as the maximum and minimum SRF applied in the probabilistic radionuclide transport modelling. For ISA, the degradation of cellulose and subsequent sorption of ISA to hydrated cement is taken into account for the maximum and minimum masses of cellulose in each repository part considered. The uncertainties in the mass of complexing agents and cellulose used to calculate the maximum and minimum SRF are discussed in Section 3.2.

Table 4-2. SRF1 (reference value, max and min).

	Ac(III); Eu(III), Am(III), Cm(III), Ho(III), Pu(III),Sm(III), Se(IV), Po(IV)			Pb(II), Pd(II)			Th(IV), Np(IV), U(IV), Pa(IV), Tc(IV), Zr(IV), Sn(IV)			Pu(IV)			U(VI), Pu(VI)		
	Reference value	Max	Min	Reference value	Max	Min	Reference value	Max	Min	Reference value	Max	Min	Reference value	Max	Min
1BMA Compartments															
1	1	1	1	1	1	1	1	1	1	1	1	1	1	1	1
2	1	1	1	100	100	100	1	1	1	1	1	1	1	1	1
3	1	1	1	100	100	100	653	2306	72	141	291	66	1	1	1
4	1	1	1	100	100	100	842	2684	81	158	326	75	1	1	1
5	1	1	1	1	1	1	20	50	5	18	46	5	1	1	1
6	1	1	1	1	1	1	1661	4322	331	233	475	112	1	1	1
7	1	1	1	100	100	100	1	1	1	1	1	1	1	1	1
8	2	3	1	100	100	100	32	74	11	29	68	10	1	1	1
9	2	2	1	100	100	100	60	422	25	56	120	23	1	1	1
10	2	3	1	100	100	100	455	1911	62	123	256	57	1	1	1
11	4	12	2	100	100	100	36	338	7	33	113	7	1	2	1
12	1	1	1	1	1	1	7	25	1	7	23	1	1	1	1
13	1	1	1	1	1	1	1	1	1	1	1	1	1	1	1
14	1	1	1	1	1	1	32	74	11	30	68	10	1	1	1
15	1	1	1	1	1	1	1	7	1	1	6	1	1	1	1
Total 1BMA structure	1	1	1	100	100	100	47	152	19	43	96	17	1	1	1
1BMA vault	1	1	1	100	100	100	13	36	2	12	33	2	1	1	1
2BMA Caissons	1	1	1	1	1	1	1	1	1	1	1	1	1	1	1
2BMA vault	1	1	1	1	1	1	1	1	1	1	1	1	1	1	1
Silo structure	1	1	1	1	1	1	179	1357	48	98	205	44	1	1	1
Silo vault	1	1	1	1	1	1	53	268	21	49	106	20	1	1	1
1BTF waste block	1	1	1	1	1	1	9	28	1	8	26	1	1	1	1
1BTF vault	1	1	1	1	1	1	1	3	1	1	3	1	1	1	1
2BTF waste block	1	1	1	1	1	1	6673	14345	2836	688	1386	340	1	1	1
2BTF vault	1	1	1	1	1	1	1788	4576	394	244	498	118	1	1	1

Table 4-3. SRF2 (reference value, max and min), and year from which it is applied (closure assumed to be year 2000). N/A indicates that the SRF is equal at all times.

	Ac(III); Eu(III), Am(III), Cm(III), Ho(III), Pu(III),Sm(III), Se(IV), Po(IV)				Pb(II), Pd(II)				Th(IV), Np(IV), U(IV), Pa(IV), Tc(IV), Zr(IV), Sn(IV)				Pu(IV)				U(VI), Pu(VI)			
	Ref SRF2	Max SRF2	Min SRF2	Time of SRF2	Ref SRF2	Max SRF2	Min SRF2	Time of SRF2	Ref SRF2	Max SRF2	Min SRF2	Time of SRF2	Ref SRF2	Max SRF2	Min SRF2	Time of SRF2	Ref SRF2	Max SRF2	Min SRF2	Time of SRF2
1BMA Compartments																				
1	1	1	1	N/A	1	1	1	N/A	1	1	1	N/A	1	1	1	N/A	1	1	1	N/A
2	1	1	1	N/A	100	100	100	N/A	1	1	1	N/A	1	1	1	N/A	1	1	1	N/A
3	1	1	1	N/A	100	100	100	N/A	1	1	1	11100	1	1	1	11100	1	1	1	N/A
4	1	1	1	N/A	100	100	100	N/A	4	4	1	11400	3	4	1	11400	1	1	1	N/A
5	1	1	1	N/A	1	1	1	N/A	1	1	1	5900	1	1	1	5900	1	1	1	N/A
6	1	1	1	N/A	1	1	1	N/A	1	1	1	12500	1	1	1	12500	1	1	1	N/A
7	1	1	1	N/A	100	100	100	N/A	1	1	1	N/A	1	1	1	N/A	1	1	1	N/A
8	2	3	1	N/A	100	100	100	N/A	17	20	1	6950	16	18	1	6950	1	1	1	N/A
9	2	2	1	N/A	100	100	100	N/A	14	16	1	8550	13	15	1	8550	1	1	1	N/A
10	2	3	1	N/A	100	100	100	N/A	17	23	1	10700	15	22	1	10700	1	1	1	N/A
11	4	12	2	N/A	100	100	100	N/A	36	338	7	N/A	33	113	7	N/A	1	2	1	N/A
12	1	1	1	N/A	1	1	1	N/A	1	1	1	4200	1	1	1	4200	1	1	1	N/A
13	1	1	1	N/A	1	1	1	N/A	1	1	1	N/A	1	1	1	N/A	1	1	1	N/A
14	1	1	1	N/A	1	1	1	N/A	1	1	1	6950	1	1	1	6950	1	1	1	N/A
15	1	1	1	N/A	1	1	1	N/A	1	1	1	N/A	1	1	1	N/A	1	1	1	N/A
1BMA structure	1	1	1	N/A	100	100	100	N/A	2	4	1	7900	2	4	1	7900	1	1	1	N/A
1BMA vault	1	1	1	N/A	100	100	100	N/A	1	3	1	5100	1	3	1	5100	1	1	1	N/A
2BMA Caissons	1	1	1	N/A	1	1	1	N/A	1	1	1	N/A	1	1	1	N/A	1	1	1	N/A
2BMA vault	1	1	1	N/A	1	1	1	N/A	1	1	1	N/A	1	1	1	N/A	1	1	1	N/A
Silo structure	1	1	1	N/A	1	1	1	N/A	1	1	1	22450	1	1	1	22450	1	1	1	N/A
Silo vault	1	1	1	N/A	1	1	1	N/A	1	1	1	17450	1	1	1	17450	1	1	1	N/A
1BTF waste block	1	1	1	N/A	1	1	1	N/A	1	1	1	2850	1	1	1	2850	1	1	1	N/A
1BTF vault	1	1	1	N/A	1	1	1	N/A	1	1	1	2400*	1	1	1	2400*	1	1	1	N/A
2BTF waste block	1	1	1	N/A	1	1	1	N/A	1	1	1	7600	1	1	1	7600	1	1	1	N/A
2BTF vault	1	1	1	N/A	1	1	1	N/A	1	1	1	6350	1	1	1	6350	1	1	1	N/A

* In the case of the 1BTF vault, only the maximum value changes over time.

5 Summary

5.1 ISA

The mass of cellulose judged to be present in many waste packages was adjusted in the recent waste inventory (SKB 2019). This has resulted in lower concentrations of ISA in these waste packages compared to those calculated in Keith-Roach et al. (2014). Overall, the total masses of cellulose in 1–2BMA, the silo and 1BTF have decreased. 2BTF and BRT do not contain cellulose, while BLA does not have a safety function relating to radionuclide sorption.

In the majority of cellulose-containing 1–2BMA waste types, the calculated ISA concentrations do not exceed the expected solubility limit for α-ISA at any time point, when sorption to the available hydrated cement (including the packaging material) has been taken into account. Following outward migration and further sorption to cement in the different compartments and waste structures of 1–2BMA, the silo and 1BTF, the dissolved ISA concentrations are reduced to a maximum of 4.2×10^{-4} M (1BMA compartment 11, 5 000 years degradation). The extrapolation of experimental cellulose degradation data from 12 to 5 000 years, and the assumption of ISA stability over this time suggest that these data are cautious.

5.2 Other complexing agents

NTA was found to have the highest concentration of the complexing agents disposed of in SFR, of up to 7.3×10^{-2} M in a waste package, and up to 2.4×10^{-3} M within a 1BMA compartment. The uncertainties associated with the NTA concentrations are a factor of 2, due to extrapolation of data relating to the use of detergents at the nuclear sites.

Citrate concentrations also were found to be relatively high, up to 5.7×10^{-3} M inside a waste package (not considering precipitation of calcium citrate) and up to 1.0×10^{-3} M in a 1BMA compartment (1BMA compartment 6). However, PhreeqC calculations suggest that precipitation of calcium citrate will limit the citrate concentration to $\sim 1 \times 10^{-3}$ M in the waste packages and that citrate will not complex radionuclides significantly in SFR.

The concentrations of all other complexing agents were found to be consistently low. Sorption of gluconate to hydrated cement and precipitation of calcium oxalate contributed to the low concentrations in the solution phase of these complexing agents in the relevant waste packages, 1BMA compartments, waste structures and vaults.

5.3 Sorption reduction factors

The largest sorption reduction factors calculated for the 1BMA compartments and 1–2BMA, the silo and 1–2BTF waste structures and vaults are associated with tetravalent radionuclides and NTA. This reflects the relatively high NTA concentrations and the strong interaction between NTA and tetravalent radionuclides, even in the presence of large amounts of Ca^{2+} from cement. Therefore, the SRF for tetravalent radionuclides derived from the NTA concentrations were often greater than those derived from the ISA concentrations.

Pb(II) and Pd(II) are frequently assigned an SRF of 100, because of the low no-effect ISA concentration (0.02 mM) and the single SRF applied above this no-effect concentration.

The SRF are consistently low for trivalent actinides and lanthanides, Se(IV), Po(IV) and hexavalent actinides. This is because only ISA is judged to affect the sorption of these radionuclides in the presence of excess portlandite, and the ISA concentrations are most often lower than the NTA concentrations.

The largest uncertainty in our current understanding of complexing agents in SFR is associated with PAN filter aid degradation. While this is being investigated further, it has not been included in the derivation of SRF. However, an additional variation case is included in the safety assessment SR-PSU (PSAR) to assess the extent to which PAN filter aid could affect the radiological doses predicted.

References

SKB's (Svensk Kärnbränslehantering AB) publications can be found at www.skb.com/publications. SKBdoc documents will be submitted upon request to document@skb.se.

Allard B, Andersson K, 1987. Chemical properties of radionuclides in a cementitious environment. SKB SFR 86-09, Svensk Kärnbränslehantering AB.

Allard B, Persson G, 1985. Organic complexing agents in low- and medium-level radioactive waste. Nagra Technical Report 85-19, Nagra, Switzerland.

Allard B, Borén H, Ephraim J, 1995. Cellulosa i cementsystem. Nedbrytningsprodukter och deras effekter på radionukliders transportegenskaper. Revised version. SKB SFR 95-01, Svensk Kärnbränslehantering AB. (In Swedish.)

Allard B, Dario M, Borén H, Torstenfelt B, Puigdomenech I, Johansson C, 2002. Karboxylatjonbytarmassans egenskaper. SKB R-02-40, Svensk Kärnbränslehantering AB. (In Swedish.)

Almkvist L, Gordon A, 2007. Low and intermediate level waste in SFR 1: Reference waste inventory 2007. SKB R-07-17, Svensk Kärnbränslehantering AB.

Altwaiq A M, Khouri S J, Abdel-Rahem R A, Alkhawaldeh A K, 2020. Conductivity method as a new monitoring technique for corrosion and corrosion Inhibition processes of zinc metal. American Journal of Analytical Chemistry 11, 349–361.

Baston G, Cowper M, Davies P, Dawson J, Farahani B, Heath T, Schofield J, Smith V, Watson S, Wilson J, 2017. The impacts of PVC additives and their degradation products on radionuclide behaviour. Radioactive Waste Management Contractor Report no. AmecFW/0006604/4, Radioactive Waste Management, UK.

Boult K, McCrohon R, Williams S J, 1998. Further experiments on the effects of Sikament 10 and Sikament N on Plutonium Solubility. RWMD(97)P95, AEA Technology, UK.

Bradbury M H, Sarott F A, 1994. Sorption databases for the cementitious near-field of a L/ILW repository for performance assessment. Nagra Technical Report 93-08, Nagra, Switzerland.

Bradbury M H, Van Loon L R, 1997. Cementitious near-field sorption data bases for performance assessment of a L/ILW repository in a Palfris host rock, CEM-94: UPDATE 1, June 1997. PSI Bericht Nr. 98-01, Paul Scherrer Institute, Switzerland.

Bruno J, González-Siso M R, Duro L, Gaona X, Altmaier M, 2018. Key master variables affecting the mobility of Ni, Pu, Tc and U in the near field of the SFR repository. Main experimental findings and PA implications of the PhD thesis. SKB TR-18-01, Svensk Kärnbränslehantering AB.

Bryan N D, Abrahamsen L, Evans N, Warwick P, Buckau G, Weng L, Van Riemsdijk W H, 2012. The effects of humic substances on the transport of radionuclides: Recent improvements in the prediction of behaviour and the understanding of mechanisms. Applied Geochemistry 27, 378–389.

Chen S, Abdel-Magied A F, Fu L, Jonsson M, Forsberg K, 2019. Incorporation of strontium and europium in crystals of α-calcium isosaccharinate. Journal of Hazardous Materials 364, 309–316.

Cronstrand P, 2016. Long-term performance of the bentonite barrier in the SFR silo. SKB TR-15-08, Svensk Kärnbränslehantering AB.

Colàs A E, 2014. Complexation of Th (IV) and U (VI) by polyhydroxy and polyamino carboxylic acids. PhD thesis. Universitat Politecnica de Catalunya, Spain.

Dario M, Molera M, Allard B, 2004. Effect of organic ligands on the sorption of europium on TiO_2 and cement at high pH. SKB TR-04-04, Svensk Kärnbränslehantering AB.

Dawson J, 2013a. NAPL Generation from the radiolysis of polyethylene and chlorosulphonated polyethylene elastomer (Hypalon®). AMEC/PPE/2834/002, AMEC, UK.

Dawson J, 2013b. The potential for non-aqueous phase liquid production from irradiated neoprene and ion-exchange resin. AMEC/PPE-000283 Issue 01, AMEC, UK.

De Windt L, Bertron A, Larreur-Cayol S, Escadeillas G, 2015. Interactions between hydrated cement paste and organic acids: Thermodynamic data and speciation modeling. Cement and Concrete Research 69, 25–36.

Duro L, Grivé M, Gaona X, Bruno J, Andersson T, Borén H, Dario M, Allard B, Hagberg J, Källström K, 2012. Study of the effect of the fibre mass UP2 degradation products on radionuclide mobilisation. SKB R-12-15, Svensk Kärnbränslehantering AB.

Ermakov I V, Rebrov A I, Litmanovich A D, Platé N A, 2000. Alkaline hydrolysis of polyacrylonitrile, 1: Structure of the reaction products. Macromolecular Chemistry and Physics 2000, 1415–1418.

Fanger G, Skagius K, Wiborgh M, 2001. Project SAFE. Complexing agents in SFR. SKB R-01-04, Svensk Kärnbränslehantering AB.

Filby A, Deissmann G, Wiegers R, 2016. LILW degradation processes and products. OPERA-PU-IBR512, COVRA, Netherlands.

García D, Grivé M, Duro L, Brassinnes S, de Pablo J, 2018. The potential role of the degradation products of cement superplasticizers on the mobility of radionuclides. Applied Geochemistry 98, 1–9.

Gaucher E, Tournassat C, Nowak C, 2005. Modelling the geochemical evolution of the multi-barrier system of the Silo of the SFR repository. Final report. SKB R-05-80, Svensk Kärnbränslehantering AB.

Giffaut E, Grivé M, Blanc P, Vieillard P, Colàs E, Gailhanou H, Gaboreau S, Marty N, Madé B, Duro L, 2014. Andra thermodynamic database for performance assessment: ThermoChimie. Applied Geochemistry 49, 225–236.

Glaus M A, Van Loon L R, 2008. Degradation of cellulose under alkaline conditions: New insights from a 12 year degradation study. Environmental Science and Technology 42, 2906–2911.

Glaus M A, Van Loon L R, 2009. Chemical reactivity of α-isosaccharinic acid in heterogeneous alkaline systems. PSI Bericht Nr 08-01, Paul Scherrer Institute, Switzerland.

Glaus M A, Van Loon L R, Achatz S, Chodura A, Fischer K, 1999. Degradation of cellulosic materials under the alkaline conditions of a cementitious repository for low and intermediate level radioactive waste: Part I: Identification of degradation products. Analytica Chimica Acta 398, 111–122.

Glaus M A, Laube A, Van Loon L R, 2003. A generic procedure for the assessment of the effect of concrete admixtures on the sorption of radionuclides on cement: Concept and selected results. Material Research Society Proceedings 807, 101–107.

Glaus M A, Laube A, Van Loon L R, 2006. Solid–liquid distribution of selected concrete admixtures in hardened cement pastes. Waste Management 26, 741–751.

González-Siso M R, Gaona X, Duro L, Altmaier M, Bruno J, 2018. Thermodynamic model of Ni(II) solubility, hydrolysis and complex formation with ISA. Radiochimica Acta 106, 31–45.

Greenfield B, Spindler M, Woodwark D, 1997. Summary of the effects of organic degradation products on near-field radionuclide chemistry. Nirex Ltd Report NSS/R298, Nirex Ltd, UK.

Hakanen M, Ervanne H, 2006. The influence of organic cement additives on radionuclide mobility: A literature survey. Posiva Working Report 2006-06, Posiva Oy, Finland.

Hedström S, 2019. Komplexbildande flyttillsatsmedel i kringgjutningsbetong i kokiller till SFR. SKBdoc 1870598 ver 1.0. Svensk Kärnbränslehantering AB. (In Swedish.)

Herterich U, Volland G, Krauser G, Hansen D, 2003. Determination of concrete admixtures in concrete by NMR spectrometry. Otto-Graf-Journal 14, 101–113.

Herterich U, Volland G, Wüstholz T, Stegmaier M, 2004. Leaching properties of self compacting concrete (SCC). Otto-Graf-Journal 15, 153–174.

Holgersson S, 2000. Studies on the effect of concrete on the chemistry in a repository for radioactive waste. PhD thesis. Department of Nuclear Chemistry, Chalmers University of Technology, Sweden.

Holgersson S, Dubois I, Börstell L, 2011. Batch experiments of Cs, Co and Eu sorption onto cement with dissolved fibre mass UP2 in the liquid phase. SKB P-11-24, Svensk Kärnbränslehantering AB.

Hummel W, 1993. Organic complexation of radionuclides in cement pore water: A case study. PSI Internal Report TM-41 -93-03, Paul Scherrer Institute, Switzerland.

Höglund L O, 2014. The impact of concrete degradation on the BMA barrier functions. SKB R-13-40, Svensk Kärnbränslehantering AB.

Johansson C, 1999a. Kemikalieinventering – Kärntekniska anläggningar. Drift PM 99/13, Reg. nr DL 721. SKBdoc 1601138 ver 1.0, Svensk Kärnbränslehantering AB. (In Swedish.)

Johansson C, 1999b. Prognos över nyttjande av SFR-1. Drift PM 99/15, Reg. Nr DL 312. SKBdoc 1601140 ver 1.0, Svensk Kärnbränslehantering AB. (In Swedish.)

Keith-Roach M, Höglund L O, 2018. Review of the long-term risks associated with the use of superplasticizers. Posiva Working Report 2017-52, Posiva Oy, Finland.

Keith-Roach M, Lindgren M, Källström K, 2014. Assessment of complexing agent concentrations in SFR. SKB R-14-03, Svensk Kärnbränslehantering AB.

Klapiszewski L, Szalaty T J, Jesionowski T, 2017. Depolymerization and activation of lignin: Current state of knowledge and perspectives. In Poletto M (ed). Lignin: trends and applications. London: IntechOpen**.**

Kobayashi T, Sasaki T, Kitamura A, 2019. Thermodynamic interpretation of uranium (IV/VI) solubility in the presence of α-isosaccharinic acid. The Journal of Chemical Thermodynamics 138, 151–158.

Kummert R, Stumm W, 1980. The surface complexation of organic acids on hydrous γ-Al_2O_3. Journal of Colloid and Interface Science 75, 373–385.

Källström K, 2013. SKB:s utlåtande kring SSM:s begäran om Komplettering av ansökan/anmälan av typbeskrivning O.01/O.02. SKBdoc 1354871 ver 3.0, Svensk Kärnbränslehantering AB. (In Swedish.)

Lagerblad B, Rogers P, Vogt C, Mårtensson P, 2017. Utveckling av konstruktionsbetong till kassunerna i 2BMA. SKB R-17-21, Svensk Kärnbränslehantering AB. (In Swedish.)

NDA, 2015. Solubility studies in the presence of PCE superplaticisers. NDA DRP Lot 2: Integrated Waste Management WP/B2/7, Nuclear Decommissioning Authority, UK.

Nixon S, Bassil, N M, Lloyd J R, 2017. Effects of radiation and microbial degradation of ILW organic polymers. Microbiology in Nuclear Waste Disposal Deliverable D1.2. EU Project 661880.

Nordén M, 1994. The complexation of some radionuclides with natural organics: Implications for radioactive waste disposal. PhD thesis. Linköping University, Sweden.

Ochs M, Talerico C, 2003. Prediction of Kd values for anion migration. Technical Report for Mitsubishi Materials Corporation, Japan.

Ochs M, Talerico C, 2004. SR-Can. Data and uncertainty assessment. Migration parameters for the bentonite buffer in the KBS-3 concept. SKB TR-04-18, Svensk Kärnbränslehantering AB.

Pavasars I, 1999. Characterisation of organic substances in waste materials under alkaline conditions. PhD thesis. Linköping University, Sweden.

Pavasars I, Hagberg J, Boren H, Allard B, 2003. Alkaline degradation of cellulose: Mechanisms and kinetics. Journal of Polymers and the Environment 11, 39–47.

Pettersson M, Elert M, 2001. Characterisation of bitumenised waste in SFR 1. SKB R-01-26, Svensk Kärnbränslehantering AB.

Pointeau I, Coreau N, Reiller P E, 2008. Uptake of anionic radionuclides onto degraded cement pastes and competing effects of organic ligands. Radiochimica Acta 96, 367–374.

Rai D, Kitamura A, 2017. Thermodynamic equilibrium constants for important isosaccharinate reactions: A review. The Journal of Chemical Thermodynamics 114, 135–143.

Rai D, Hess N J, Xia Y, Rao L, Cho H M, Moore R C, Van Loon L R, 2003. Comprehensive thermodynamic model applicable to highly acidic to basic conditions for isosaccharinate reactions with Ca(II) and Np(IV). Journal of Solution Chemistry 32, 665–689.

Rai D, Yui M, Moore D A, Rao L, 2009. Thermodynamic model for $ThO_{2(am)}$ solubility in iso-saccharinate solutions. Journal of Solution Chemistry 38, 1573–1587.

Rébufa C, Traboulsi A, Labed V, Dupuy N, Sergent M, 2015. Experimental design approach for identification of the factors influencing the γ-radiolysis of ion exchange resins. Radiation Physics and Chemistry 106, 223–234.

Reinoso-Maset E, Worsfold P J, Keith-Roach M J, 2012. The effect of EDTA, NTA and picolinic acid on Th(IV) mobility in a ternary system with natural sand. Environmental Pollution 162, 399–405.

Rizoulis A, Steele H M, Morris K, Lloyd J R, 2012. The potential impact of anaerobic microbial metabolism during the geological disposal of intermediate-level waste. Mineralogical Magazine 76, 3261–3270.

Rojo H, Tits J, Gaona X, Garcia-Gutierrez M, Missana T, Wieland E, 2013. Thermodynamics of Np(IV) complexes with gluconic acid under alkaline conditions: sorption studies. Radiochimica Acta 101, 133–138.

Ruckstuhl S, Suter M J F, Kohler H P E, Giger W, 2002. Leaching and primary biodegradation of sulfonated naphthalenes and their formaldehyde condensates from concrete superplasticizers in groundwater affected by tunnel construction. Environmental Science & Technology 36, 3284–3289.

Shaw P E, Tatum J H, Berry R E, 1969. Base-catalyzed sucrose degradation studies. Journal of Agricultural Food Chemistry 17, 907–908.

SKB, 1991. SFR-1. Fördjupad Säkerhetsanalys. SKB SFR 91-10, Svensk Kärnbränslehantering AB. (In Swedish.)

SKB, 2013. Låg- och medelaktivt avfall i SFR – Referensinventarium för avfall 2013. SKB R-13-37, Svensk Kärnbränslehantering AB. (In Swedish.)

SKB, 2014a. Data report for the safety assessment SR-PSU. SKB TR-14-10, Svensk Kärnbränslehantering AB.

SKB, 2014b. Waste form and packaging process report for the safety assessment SR-PSU. SKB TR-14-03, Svensk Kärnbränslehantering AB.

SKB, 2018. Initial state report SR-PSU (PSAR). Datafrys 1 – indata till hydrologiska beräkningar. SKBdoc 1671641 ver 1.0, Svensk Kärnbränslehantering AB. (In Swedish.)

SKB, 2019. Låg- och medelaktivt avfall i SFR: Referensinventarium för avfall 2016. SKB R-18-07, Svensk Kärnbränslehantering AB. (In Swedish.)

Studsvik Nuclear, 2018. PM – Komplexbildande ämnen i avfall tillhörande S.09. S-18/195. Studsvik Nuclear AB. SKBdoc 1701211 ver 1.0, Svensk Kärnbränslehantering AB. (In Swedish.)

Tasi A, 2018. Solubility, redox and sorption behavior of plutonium in the presence of α-D-isosaccharinic acid and cement under reducing, alkaline conditions. PhD thesis. Karlsruhe Institute of Technology, Germany.

Van Loon L R, Glaus M A, 1997. Review of the kinetics of alkaline degradation of cellulose in view of its relevance for safety assessment of radioactive waste repositories. Journal of Environmental Polymer Degradation 5, 97–109.

Van Loon L R, Glaus M A, 1998. Experimental and theoretical studies on alkaline degradation of cellulose and its impact on the sorption of radionuclides. PSI Bericht Nr 98-07, Paul Scherrer Institute, Switzerland. Nagra Technical Report NTB 97-04, Nagra, Switzerland.

Van Loon L R, Hummel W, 1995. The radiolytic and chemical degradation of organic ion exchange resins under alkaline conditions: effect on radionuclide speciation. PSI-Bericht 95-13, Paul Scherrer Institute, Switzerland. Nagra Technical Report NTB 95-08, Nagra, Switzerland.

Van Loon L R, Hummel W, 1999a. Radiolytic and chemical degradation of strong acidic ion-exchange resins: Study of the ligands formed. Nuclear Technology 128, 359–371.

Van Loon L R, Hummel W, 1999b. The degradation of strong basic anion exchange resins and mixed-bed ion exchange resins: Effect of degradation products on radionuclide speciation, Nuclear Technology 128, 388–401.

Van Loon L R, Glaus M A, Stallone S, Laube A, 1997. Sorption of isosaccharinic acid, a cellulose degradation product, on cement. Environmental Science & Technology 31, 1243–1245.

Van Loon L R, Glaus M A, Laube A, Stallone S, 1999a. Degradation of cellulosic materials under the alkaline conditions of a cementitious repository for low- and intermediate-level radioactive waste. Part II: Degradation kinetics. Journal of Environmental Polymer Degradation 7, 41–51.

Van Loon L R, Glaus M A, Laube A, Stallone S, 1999b. Degradation of cellulosic materials under the alkaline conditions of a cementitious repository for low- and intermediate-level radioactive waste. Part III: Effect of the degradation products on the sorption of radionuclides on feldspar. Radiochimica Acta 84, 221–224.

von Schenck H, Källström K, 2013. Reactive transport modelling of organic complexing agents in cement stabilized low and intermediate level waste. Physics and Chemistry of the Earth, Parts A/B/C 70–71.

Wang L, Martens E, Jacques D, de Cannière P, Berry J, Mallants D, 2009. Review of sorption values for the cementitious near field of a near surface radioactive waste disposal facility. NIROND TR 2008-23E, ONDRAF/NIRAS, Belgium.

Warwick P, Evans N, Hall T, Vines S, 2003. Complexation of Ni(II) by alpha iso-saccharinic acid and gluconic acid from pH 7 to pH 13. Radiochimica Acta 91, 233–240.

Warwick P, Evans N, Hall T, Vines S, 2004. Stability constants of uranium(VI)-alpha-isosaccharinic acid and gluconic acid complexes. Radiochimica Acta 92, 897–902.

Wieland E, Tits J, 2002. The effect of α-isosaccharinic acid on the stability of and Th(IV) uptake by hardened cement paste. Radiochimica Acta 90, 683–688.

Wieland E, Tits J, Spieler P, Dobler J P, 1998. Interaction of Eu(III) and Th(IV) with sulphate-resisting Portland cement. Material Research Symposium Proceedings 506, 573–578.

Wieland E, Lothenbach B, Glaus M A, Thoenen T, Schwyn B, 2014. Influence of superplasticizers on the long-term properties of cement pastes and possible impact on radionuclide uptake in a cement-based repository for radioactive waste. Applied Geochemistry 49, 126–142.

Wold S, 2003. On diffusion of organic colloids in compacted bentonite. PhD thesis. Royal Institute of Technology, Sweden.

Yamamoto T, Nishida T, Hironaga M, Suzuki S, Ueda H, 2008. Release of superplasticizers and other organic additives from altered cement. NUMO-TR-08-01, Nuclear Waste Management Organization of Japan.

Appendix 1

Materials present in SFR wastes

Table A1-1. Materials reported to be present in SFR waste packages by the waste producers[7]. Some materials are reported in different ways, e.g. cellulose is sometimes reported as cellulose or as the material that is composed of cellulose (e.g. paper).

Material present in SFR waste packages	Organic content	Degradation discussed in Section 2.2?	Comment
Aluminium	None	No	Inorganic
Asbestos (other inorganic)	None	No	Inorganic
Ash	None	No	Inorganic
Bitumen	Complex organic mixture	Section 2.2.4	
Cellulose (mainly from paper, cloth and wood)	Cellulose	Section 2.2.1	
Cement	Cement additives		See “cement additives” below
Cement additives (inorganic)	None	No	
Cement additives (organic)	Organic molecules and polymers	Section 2.2.7	See Table 2-1
Cloth	Dry weight assumed to be 100 % cellulose (conservative)	Section 2.2.1	Cellulose
Concrete	Cement additives		See “cement additives” above
Emulsifier (other inorganic)	None	No	Inorganic
Ethafoam (plastic)	Polyethylene	Section 2.2.6	
Evaporates	Low	No	Mainly inorganic
Filter aid	Inorganic or organic. UP2 is a polymer $[C_3H_3N]_n$. Can contain cellulose (e.g. F.05, F.15)	Sections 2.2.3 and 2.2.1	
Flocculants (other inorganic)	None	No	Inorganic
Frigolite	Plastic	Section 2.2.6	
Glycol	Non-complexing cement additive	No	Non-complexing
Inorganic complexing agents	None (e.g. $CaCO_3$)	No	Inorganic
Ion exchange resins	Amine, sulfonic acid and carboxylate functional groups	Section 2.2.5	
Iron/steel	None	No	Inorganic
Lead	None	No	Inorganic
Lime (other inorganic)	None	No	Inorganic
Metal hydroxides (other inorganic)	None	No	Inorganic
Organic complexing agents	Organic structures	No	Not expected to degrade
Other inorganic materials	None	No	Inorganic
Other organic materials	Yes	No	Uncharacterised
Paper	Assumed to be 100 % cellulose (conservative)	Section 2.2.1	
Plastic	Mainly polyethylene and polystyrene	Section 2.2.6	
Rubber	Composed of C and H	Section 2.2.6	
Sand (other inorganic)	None	No	Inorganic
Silix GP (other inorganic)	None (SiO_2)	No	Inorganic
Sika Aer (other inorganic)	None (SiO_2)	No	Inorganic
Sludge	Can contain detergents, but mainly metal hydroxides	No	Complexing agents from detergents assessed separately
Sodium sulfate (other inorganic)	None	No	Inorganic
Water sealant (other inorganic)	None	No	Inorganic
Wood (cellulose)	Cellulose 80 %	Section 2.2.1	
Wood (other organic)	Lignin 20 %	Section 2.2.2	
Zinc	None	No	Inorganic

[7] Barsebäck, CLAB, Cyclife, Forsmark, Ringhals, Oskarshamn, Studsvik Nuclear, SVAFO.

Appendix 2

Mass of complexing agents in SFR

The estimation of the mass of complexing agents present in SFR from each nuclear facility is described in this Appendix, and the total masses in SFR are given. First, the estimated mass of EDTA in SFR is presented, and then each nuclear facility is considered in turn. The estimates mainly reflect wastes produced up to the end of 2012, i.e. up to the implementation of new SFR waste acceptance criteria with restrictions of the mass of complexing agents (Almkvist 2012). The number of waste packages produced that are considered to contain complexing agents are given in Table A2-1.

Table A2-1. Number of waste packages considered to contain complexing agents.

Vault	Waste type	Number of waste packages assumed to contain EDTA	Number of waste packages considered to contain other complexing agents
Silo	B.04	0	349
	C.02	0	416
	O.02	0	346
	R.16	664	1445
1BMA	F.17	352	608
	R.10	84	84
	R.15	147	147
2BMA	S.09 (3 variants)	611 (555 + 56)	715 (555 + 56 + 104)
BTF	B.07/B.07.01	212	212/11
	O.07/ O.07:00	378	378

EDTA

EDTA was used at the Swedish nuclear facilities until 1998, when EDTA was banned in waste destined for SFR. Fanger et al. (2001) reported that SKB had estimated that a maximum of 10 kg EDTA has been disposed of in SFR. This mass was assumed to arise equally from each of the four nuclear power facilities in Sweden. Since then it has also been identified that small amounts of EDTA were also used at Studsvik Nuclear AB and, as described in the relevant section below, this adds a further 5.2 kg to the total mass of EDTA in SFR. Therefore, 15.2 kg of EDTA are present in SFR.

A2.1 Barsebäck

The main source of strong complexing agents in the SFR waste from Barsebäck is liquid floor cleaner (ca 225 L/a)[8]. Nilfisk Industri Kombi was used until 2003, containing 0.5 % NTA and Induren A was used from 2003 to 2010, containing 3 % sodium gluconate (and 1–2 % sodium iminodisuccinate). Ikanol Plus Special has been used since January 2011, which does not contain strong complexing agents[3].

A low proportion of the complexing agents used has been found to accumulate in the B.07 concrete tanks. In the period 2003–2005, it was found to be only 0.25 % [3]. As a result, only 0.28 kg of sodium gluconate is present in the 10 packages of B.07.01 produced between 2003 and 2010 and 0.309 kg in one B.07.01 package produced after this[3]. In total, 0.59 kg of sodium gluconate from Barsebäck has been disposed of in SFR.

Sodium iminodisuccinate is an amino tetracarboxylic acid and is therefore expected to be a strong complexing agent. However, the concentration of sodium gluconate in B.07 is calculated to be 1.2×10^{-4} M in 11 waste packages (no sorption) and the concentration of sodium iminodisuccinate would be lower than this, as it is present at a lower concentration in Induren A and has a higher molecular mass. There is therefore no need to consider this small mass of sodium iminodisuccinate further.

[8] **Håkansson L, 2011.** Underlagsrapport för typbeskrivning B.07.1. Barsebäck dokument 2117789/2.0, Barsebäck Kraft AB, Sweden. (In Swedish.) (Internal document.)

The mass of NTA in B.07 waste packages was estimated from the 225 L/a of Nilfisk Industri Kombi used before 2003, assuming that 112.5 L/a was used for 24 years at reactor B1 and 28 years at reactor B2. The percentage of NTA that accumulated in B.07 concrete tanks was assumed to be equal to that of gluconate in the period 2003–2005, i.e. 0.25 %[9]. The total volume of Nilfisk Industri Kombi used is therefore 5 850 L, which contained 29.3 kg of NTA, of which 0.073 kg NTA accumulated in B.07 concrete tanks.

In addition to this, Barsebäck have estimated that 40 kg oxalate has been used for system decontamination and that this was disposed of in the B.04 waste packages produced before 2010.

3.8 kg of citric acid was used at Barsebäck in 1998 (Johansson 1999a). To extrapolate this over time, 3.8 kg was divided into the 15 B.07 waste packages produced annually (Johansson 1999b) and multiplied by the 212 B.07 waste packages produced that contain organic complexing agents (Table A2-1). This suggests that a total of 53 kg citrate from Barsebäck has been disposed of in SFR. This approach is consistent with Fanger et al. (2001) and Keith-Roach et al. (2014) but is conservative as it does not take into account that only a small proportion of complexing agents are expected to have accumulated in the B.07 waste packages.

The estimated mass of complexing agents in SFR from Barsebäck is summarised in Table A2-2.

Table A2-2. Estimated mass of complexing agents (kg) in SFR from Barsebäck.

Waste type	EDTA	NKP	NTA	Citrate	Oxalate	Sodium gluconate
B.04					40	
B.07	2.5		0.073	53		
B.07.01						0.59
Total	**2.5**	**0**	**0.073**	**53**	**40**	**0.59**

A2.2 Clab

Clab came into operation in 1985. Information was provided on their use of detergents in 2009:

- 200 L Nordex Industrikombi (discontinued December 2011) containing max 0.5 % NTA.
- 5 L Grovrent containing 0.35 % NTA.

The mass of NTA in these detergents was divided into the number of C.02 waste packages produced annually (15; Almkvist and Gordon 2007) and multiplied by the 416 C.02 waste packages produced that contain complexing agents (Table A2-1). This is summarised in Table A2-3.

Table A2-3. NTA from the detergents used at Clab in 2009 and extrapolation to the mass in SFR.

Detergent	NTA (%)	Volume used in 2009 (L)	NTA used in 2009 (kg)	NTA (kg) per C.02 package	NTA (kg) to SFR
Nordex Industrikombi	0.5	200	1	0.0667	27.7
Grovrent	0.35	5	0.0175	0.00117	0.49
Total					**28.2**

A2.3 Forsmark

The waste conditioning facility at Forsmark has been in operation since 1987. Information was provided on the mass or volume of chemicals taken from the main store from 2000 to 2011, while the annual environmental reports (1987–2011) were used to assess the mass of detergents used on-site by the facility management company. Quantitative data were available for certain periods

[9] **Håkansson L, 2011.** Underlagsrapport för typbeskrivning B.07.1. Barsebäck dokument 2117789/2.0, Barsebäck Kraft AB, Sweden. (In Swedish.) (Internal document.)

of the operational phase. Therefore, when no other information was available, it was assumed that the detergent was used in the same quantity every year over the period 1987–2012. The calculations of the total masses used at Forsmark are shown in Table A2-4 and Table A2-5. It is assumed that all liquid detergents have a density of 1 kg/L.

Detergents and chemicals used at Forsmark are only disposed of in SFR if they were used in the active areas and if the wastewater was evaporated to produce a solid waste for disposal. Table A2-6 shows the percentage of each detergent estimated to be used in the active areas of Forsmark and, as a result, on the total mass used in these areas. The average use per year in the active areas was then calculated (typically 25 years use; exceptions shown in Table A2-5).

The detergent was assumed to be used equally at each of the three reactors, F1, F2 and F3. All detergents used at F3 are assumed to be disposed of in SFR since all wastewater was evaporated under the operational period. The percent of the water that was evaporated at F1 and F2 changed over time:

F1 and F2: Before 1989: 0 %

1989–2003: 10 %

2004–2006: 50 %

2007–2012: 100 %

The masses of complexing agents destined for SFR are shown in Table A2-6, taking these changes into account.

Table A2-4. Mass of chemicals taken from the main store at Forsmark and extrapolation to the mass used in the period 1987–2012.

Name	Packet size (kg)	Number of packets	Use start	Use end	Total mass used (kg)	Time of use (months)	Factor to account for 300 months operation	Total mass 1987–2012 (kg)
Nordex Industrikombi	5	10744	Feb 2001	Dec 2011	53720	131	2.29	123000
Sumatox LpH DEKO	10	33	Dec 2001	May 2011	330	114	2.63	868
Vattenbaserad avfettning ST409	25	28	Sep 2000	July 2009	700	104	2.88	2020
Absorptionsmedel ABSOL	40	999	Sep 2000	Dec 2011	39960	136	2.21	88100
Citric acid 1-hydrate	5	30	Dec 2002	Dec 2010	150	97	3.09	464
Oxalic acid 2-hydrate	0.5	23	May 2002	May 2011	12	109	2.75	32

Table A2-5. Mass of detergents used by Forsmark's facility management company 2004–2009 and extrapolation to the entire period in which the detergent was used.

Name	Average use 2004–2009 (kg/a)	Period of use	Time used (a)	Total mass during period of use (kg)
Putsväck (grovtvål)	240	2006–2011	6	1440
Mevon 66 (flytande duschtvål, efter 2006 IKO)	775	1987–2005	19	14700
Mevon 77 (flytande tvål)	1111	1987–2011	25	27800
Suma alu free	1550	2006–2011	5.3	8200

Table A2-6. Mass of detergents used in active areas and conversion to the mass of complexing agents in SFR. The calculations take into account changes in the percentage of the water evaporated over time.

Product	Used in active areas (%)	Total used in active areas (1987–2012)	Average annual use in active areas (kg/a)	Mass to SFR from F1 and F2 up to the end of 2011 (kg)	Mass to SFR from F3 up to the end of 2011 (kg)	Complexing agent content	Mass of complexing agent to SFR (kg)
Nordex Industrikombi	70	86 116	3 445	18 400	28 700	0.5 % NTA	235
Sumatox LpH DEKO	70	608	24	130	203	15 % NTA	50
Vattenbaserad avfettning ST409	70	1 413	57	301	471	3 % Na-gluconate	23
Absorptions-medel ABSOL	70	61 703	2 468				
Citronsyra 1-hydrat	70	325	13	70	108	100 % citrate	178
Oxalsyra 2-hydrat	70	22	0.89	5	7.5	100 % oxalate	12.5
Putsväck (grovtvål)	25	360	60	220	120	0.9 % citrate	3.1
Mevon 66 (flytande duschtvål, efter 2006 IKO)	5	736	39	65	245	1 % citrate	3.1
Mevon 77 (flytande tvål)	25	6 946	278	1 480	2 310	1 % citrate	38
Suma alu free	100	8 215	1 550	4 960	2 740	3 % MGDA*	231

* MGDA is structurally similar to NTA and considered together with NTA.

The estimated mass of complexing agents in SFR from Forsmark is summarised in Table A2-7.

Table A2-7. Estimated mass of complexing agents (kg) in SFR from Forsmark.

Waste type	EDTA (kg)	NKP (kg)	NTA incl. MGDA (kg)	Citrate (kg)	Oxalate (kg)	Sodium gluconate (kg)
F.17	2.5	0	516	222	12.5	23
Total	**2.5**	**0**	**516**	**222**	**12.5**	**23**

A2.4 Oskarshamn

The complexing agents used routinely at Oskarshamn are disposed of in waste packages of type O.07. By the end of 2016, 606 O.07 waste packages had been produced.

Through communication with Oskarshamn, SKB has become aware that the previous assessment of the complexing agent content of washing detergents used at Oskarshamn was based on the safety data sheets for the products, which do not name the relevant complexing agents. The previous assessments of the masses of complexing agents present in O.07 waste packages have therefore been superseded by a recent assessment of detergent use at Oskarshamn over time and the expected accumulation of complexing agents in O.07 waste packages[10]. In total, 378 O.07 are judged to contain MGDA, citrate and/or an unknown carboxylate amine (assumed here to be NKP, as identified in Fanger et al. (2001)), but the masses of complexing agents varied over time. The amounts are summarised in Table A2-8.

[10] **Hedström S, Bultmark F, Sihm Kvenangen K, 2019.** Konsekvensutredning – Komplexbildare i avfallstyper O.07 och F.17 och deras påverkan på säkerhet efter förslutning. SKBdoc 1877287 ver 3.0, Svensk Kärnbränslehantering AB. (In Swedish.) (Internal document.)

Table A2-8. Complexing agents in waste type O.07 over time.

Time period	Block	Product	Complexing agent	Mass of each complexing agent (kg/waste package)	Number of waste packages disposed of in 1BTF	Number of waste packages disposed of in 2BTF
1976–1993	O1	Laundry detergent	MGDA and citrate	3.87	12	259
1987–1993	O3	Laundry detergent	MGDA and citrate	10.5	3	34
1993–2009	O3	Laundry detergent	MGDA and citrate	40.1	0	49
2010–2019	O3	Laundry detergent	MGDA and citrate	0.0067	4	8
2014–2019		OKG-rent	Carboxylated amine	5.18	10	3
Number with both OKG-rent and laundry detergent					3	1
Total number					26	352

The total mass of complexing agents arising from this waste is summarised in Table A2-9, assuming that no more than the 13 waste packages containing OKG-rent that have already been disposed of will be disposed of in SFR. A total of 32 packages were produced containing OKG-rent[11].

Oxalate was used on 16 occasions between 1990–2010 during system decontamination at Oskarshamn, and this was disposed of in O.02 type waste packages (Källström 2013). The total mass used is estimated to be 50 kg and, as it was only used occasionally, it was judged to have been divided into a limited number of O.02 waste packages (Table A2-1). The estimated mass of complexing agents in SFR from Oskarshamn is summarised in Table A2-9.

Table A2-9. Estimated mass of complexing agents (kg) in SFR from Oskarshamn. The carboxylated amine is assumed to be NKP.

Waste type	EDTA (kg)	Carboxylated amine (kg)	NTA/MGDA (kg)	Citrate (kg)	Oxalate (kg)	Sodium gluconate (kg)
O.02					50	
O.07	2.5	67	3400	3400		0
Total	**2.5**	**67**	**3400**	**3400**	**50**	**0**

A2.5 Ringhals

Detergents containing complexing agents were used in the Ringhals decontamination and sanitation facilities from 1976 to 2010. Although all of the complexing agents in the detergents used in the sanitation facilities were sent to SFR, those used at the decontamination facility before 2004 were not sent to SFR.

[11] **Hedström S, Bultmark F, Sihm Kvenangen K, 2019.** Konsekvensutredning – Komplexbildare i avfallstyper O.07 och F.17 och deras påverkan på säkerhet efter förslutning. SKBdoc 1877287 ver 3.0, Svensk Kärnbränslehantering AB. (In Swedish.) (Internal document.)

The masses of detergents used in Ringhals decontamination facility in 2002 are shown in Table A2-10,[12] together with an estimation of the mass used over the time when the material was destined for SFR.

Table A2-10. Complexing agents from Ringhals decontamination facility sent to SFR.

Product	Complexing agent content	Period to SFR	Use in 2002 (kg/a)	Proportion to SFR	Complexing agents to SFR (kg/a)	Total mass of complexing agent to SFR (kg)
Induren A (1981–2005)	5 % NTA	2004–2005	160	1	8	8
Induren A (2005–2010)	3 % sodium gluconate	2005–2010	160	1	4.8	24
Sumatox LPH-dekont	15 % NTA	2004–2010	106	1	16	95

The masses of detergents used in Ringhals' sanitation facilities in 2002 that will accumulate in wastes destined for SFR[13] were extrapolated to the entire operational period (Table A2-11). The main relevant product was Induren A, which contained 5 % NTA up to 2005 and 3 % sodium gluconate afterwards.

Table A2-11. Complexing agents from Ringhals sanitation facilities sent to SFR. Induren A was used throughout the relevant period but the recipe changed in 2005.

Facility (time period)	Complexing agent content of product	Period to SFR	Use in 2002 (kg/a)	Proportion to SFR	Complexing agents to SFR (kg/a)	Total mass complexing agent to SFR (kg)
Waste (1981–2005)	5 % NTA	1981–2005	64	1	3	77
Waste (2005–2011)	3 % sodium gluconate	2006–2010	64	1	2	8
R1 (1981–2005)	5 % NTA	1976–2005	585	0.5	15	424
R1 (2005–2011)	3 % sodium gluconate	2006–2010	585	0.5	9	35
R2 (1981–2005)	5 % NTA	1976–2005	250	1	13	363
R2 (2005–2011)	3 % sodium gluconate	2006–2010	250	1	8	30
R3 (1980–2005)	5 % NTA	1980–2005	215	1	11	258
R3 (2005–2011)	3 % sodium gluconate	2006–2010	215	1	6	26
R4 (1981–2005)	5 % NTA	1982–2005	188	1	9	216
R4 (2005–2011)	3 % sodium gluconate	2006–2010	188	1	6	23
Total NTA						**1 340**
Total sodium gluconate						**121**

[12] **Möller J, Torstenfelt B, 2003.** Behandling av aktivt vatten med inblandning av kemikalier från all vattenhantering. SwedPower dokumentnummer T-SEKV 2003-023, SwedPower, Sweden. (In Swedish.) (Internal document.)

[13] **Möller J, Torstenfelt B, 2003.** Behandling av aktivt vatten med inblandning av kemikalier från all vattenhantering. SwedPower dokumentnummer T-SEKV 2003-023, SwedPower, Sweden. (In Swedish.) (Internal document.)

The estimated mass of complexing agents from Ringhals in SFR is summarised in Table A2-12. The complexing agents were divided into the R.10, R.15 and R.16 waste packages produced in the relevant time period (Table A2-1).

Table A2-12. Estimated mass of complexing agents (kg) in SFR from Ringhals.

Source	EDTA	NTA	Sodium gluconate
Decontamination facility		100	24
Sanitation facilities		1300	120
Unspecified	2.5		
Total	**2.5**	**1400**	**150**

A2.6 Studsvik Nuclear AB and SVAFO

Studsvik Nuclear AB and SVAFO produce waste type S.09 that is destined for 2BMA. A recent memo (Studsvik Nuclear 2018) estimated that waste type S.09 produced up to the end of 2006 contained 9 g EDTA and 9 g NTA, and 9 g NTA from 2007 onwards. This was based on the mass of detergents used, although the assumption that NTA was the complexing agent was conservative.

The mass of complexing agents in 56 waste packages was determined separately and contained 4.3 g of EDTA and 3 g of sodium gluconate. In total, 715 S.09 waste packages will be disposed of in 2BMA and these are divided up as follows: 56 with determined complexing agent concentrations, 555 other S.09 packages produced before the end of 2006 and 104 produced from the beginning of 2007.

The estimated mass of complexing agents from Studsvik Nuclear and SVAFO in SFR is summarised in Table A2-13.

Table A2-13. Estimated mass of complexing agents (kg) in SFR from Studsvik Nuclear and SVAFO.

Type of S.09	Number	EDTA (kg)	NTA (kg)	Sodium gluconate (kg)
Complexing agent concentration determined	56	0.24		0.17
Other S.09 produced before the end of 2006	555	5	5	
Produced from the beginning of 2007	104		0.94	
Total (kg)		**5.2**	**5.9**	**0.17**

A2.7 Total mass of complexing agents in SFR

The estimated mass of complexing agents to be disposed of in SFR is summarised in Table A2-14.

Table A2-14. Summary of the total mass of complexing agents (kg) disposed of in SFR (to 2 significant figures).

Nuclear facility	EDTA	NKP	NTA	Citrate	Oxalate	Sodium gluconate
Barsebäck	2.5	-	0.073	53	40	0.59
Clab	0	-	28	-	-	-
Forsmark	2.5	-	520	220	12	23
Oskarshamn	2.5	67	3400	3400	50	-
Ringhals	2.5	-	1400	-	-	150
Studsvik	5.2	-	5.9	-	-	0.17
Total	**15**	**67**	**5400**	**3700**	**100**	**170**

Appendix 3

PhreeqC modelling of Dario's experiments and extrapolation to SFR conditions

A3.1 Introduction

Modelling calculations (Hummel 1993) suggested that EDTA, NTA, citrate and oxalate do not form complexes with a wide range of radionuclides in cement porewater of pH 11–13 with Ca concentrations from 1 mM to 100 mM. EDTA alone had an effect and only on Mn, Ni and Pb. In all other cases Ca-complexing agent or metal-hydroxide complexes formed. Speciation databases have developed a great deal since 1993, which means the results of similar calculations may now be different.

The effect of Ca^{2+} on Eu(III) complexation by organic complexing agents was observed in the experiments of Dario et al. (2004), where NTA (see Figure A3-1) and EDTA did not affect Eu(III) sorption to 1 g/L cement or TiO_2 with added Ca^{2+} until all Ca^{2+} was complexed. NTA reduced Eu(III) sorption to TiO_2 at lower concentrations in the absence of Ca^{2+} because of this. The addition of citrate reduced sorption to a lesser but still significant extent, and the importance of Ca^{2+} could be seen (Figure A3-1).

ISA, on the other hand, began to affect Eu(III) sorption in the three systems investigated at very similar concentrations and the gradients were similar (Figure A3-2). This suggests that Ca^{2+} has little impact on the effect of ISA on Eu(III) sorption

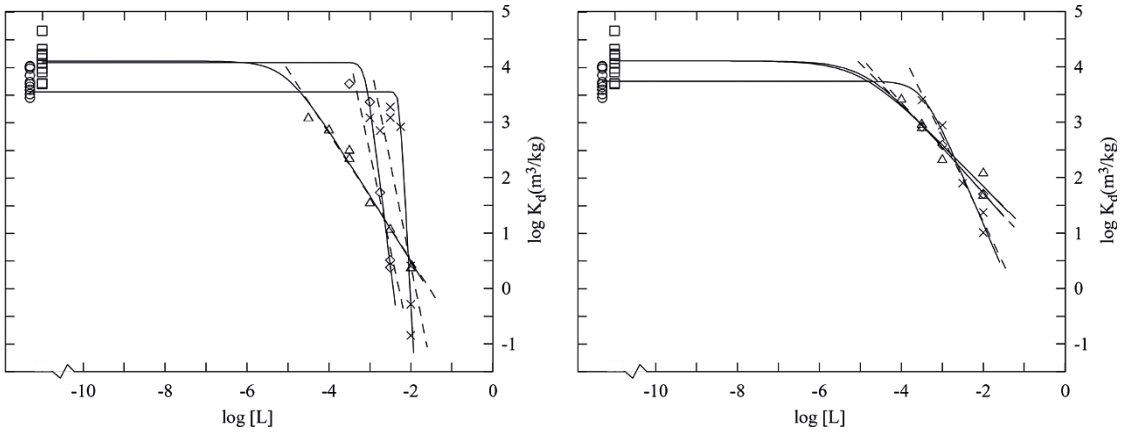

Eu sorption with L = NTA, (□) TiO_2, [L] = 0 M, (○) Cement, [L] = 0 M, (Δ) TiO_2, (◊) TiO_2, [Ca] = 0.002 M, (x) Cement

Eu sorption with L = citric acid, (□) TiO_2, [L] = 0 M, (○) Cement, [L] = 0 M, (Δ) TiO_2, (◊) TiO_2, [Ca] = 0.002 M, (x) Cement

Figure A3-1. *Effect of NTA (left) and citrate (right) on Eu(III) sorption to cement and TiO_2 (Dario et al. 2004). Eu(III) was added at a concentration of 10^{-8} M.*

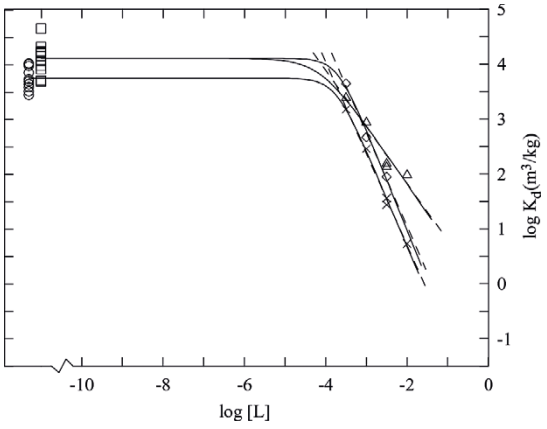

Eu sorption with L = ISA, (□) TiO_2, [L] = 0 M, (○) Cement, [L] = 0 M, (Δ) TiO_2, (◊) TiO_2, [Ca] = 0.002 M, (x) Cement

Figure A3-2. *Effect of ISA on Eu(III) sorption to cement and TiO_2 (Dario et al. 2004). Eu(III) was added at a concentration of 10^{-8} M.*

The influence of Ca^{2+} on the effect of EDTA and NTA was previously included in the data selection for SR-PSU (SKB 2014a) as follows, "Because of the strong competition of Ca for complexation by these compounds, it appears as a first approximation that their effect on radionuclide sorption is only relevant when their concentration exceeds the dissolved concentration of Ca (Dario et al. 2004). In detail, the effect will depend on the stabilities of all relevant species in the RN-EDTA-Ca-HCP system. The dissolved Ca concentration in equilibrium with portlandite and other HCP minerals can be estimated as approximately 1 mM (states I and III) to 10 mM (state II), depending on conditions (see e.g. Wang et al. 2009)."

While this argument is reasonable, it does not appear to have been investigated further and it does not address the effect of Ca^{2+} complexation on the equilibrium between portlandite and dissolved Ca^{2+}, i.e. enhanced dissolution of portlandite. Dario et al. (2004) carried out experiments with 1 g/L HCP, and so the concentration of portlandite available for dissolution was a fraction of the concentration available in cement or concrete porewater.

In order to see the effect of increasing the concentration of available portlandite on speciation, calculations have been carried out in PhreeqC using Version 9 of the ThermoChimie database (Giffaut et al. 2014). Am(III) was used as an analogue of Eu(III), due to the more complete data in the ThermoChimie database, together with a variety of complexing agents relevant to SFR. Additional cases have also been run with a) Eu to compare with the Am results and b) Th(IV) to examine the effect of ISA, NTA and citrate on tetravalent actinides (in concrete porewater only).

A3.2 Method

Based on estimates presented by Höglund (2014), the content of free portlandite in fully hydrated cement was assumed to be 2.96 mol $Ca(OH)_2$ per kg of dry cement clinker. Assuming a water:cement ratio of 0.4, this was equivalent to 2.1 mol $Ca(OH)_2$ per kg of HCP.

Concrete is assumed here to consist of 350 kg dry cement clinker/m^3, and have a density of 2 450 kg/m^3. Hence, the free portlandite content of concrete amounts to 0.42 mol/kg. Since 1 L of concrete has a mass of 2.45 kg, the portlandite concentration is 1 M.

The F.17 and R.10 waste packages contain the highest concentrations of NTA. F.17 is bitumen conditioned while R.10 contains 1 400 kg of hydrated cement in the waste, cement conditioning and container, and has a volume of 1.728 m^3, i.e. 0.81 kg hydrated cement/L, or 1.7 mol portlandite/L. Radionuclide sorption to bitumen is negligible and so complexation of radionuclides present in F.17 waste packages is most relevant when considering 1BMA at a compartment level. Compartment 6 contains the highest number of F.17 packages, and so is considered here. Compartment 6 contains $\sim 4 \times 10^5$ kg of hydrated cement (including the structural concrete) and has a total volume of 1 468 m^3, i.e. 0.28 kg hydrated cement/L. or 0.59 mol portlandite/L. The portlandite concentration in concrete is therefore a reasonable representation of that in R.10 and Compartment 6.

Calculations were carried out for a variety of radionuclide-complexing agent combinations (see Table A3-1) in:

1. Water in equilibrium with 1 g/L HCP solid phase (0.0021 mol $Ca(OH)_2$/L) "experimental conditions".
2. Water in equilibrium with 2.45 kg/L concrete solid phase (1 mol $Ca(OH)_2$/L) "concrete porewater".

In both cases, the radionuclide concentration was 10^{-8} M, for consistency with Dario et al. (2004), the initial pH was pH 12.6, the temperature was 15 °C and the charge was balanced on Na^+, which had an initial concentration 2.2×10^{-2} M. The complexing agent was titrated into the mixture in 100 steps, up to a maximum of 10^{-2} M. The species and solid phases included in Thermochimie_v9 and in the calculations are shown in Table A3-1).

Table A3-1. Species included in the Thermochimie_v9 database for each combination of radionuclide and complexing agent investigated. The dominant member of each group of species under the conditions of the calculations is shown in bold.

Radionuclide	Complexing agent	Radionuclide-complex species	Ca complex species	Solid phases
Am(III)	NTA	Am(NTA) **$Am(NTA)_2^{3-}$**	**$Ca(NTA)^-$** Ca(HNTA) $Ca(HNTA)_2^{2-}$	
Am(III)	Citrate	Am(Cit) **$Am(Cit)_2^{3-}$** $Am(HCit)^+$ $Am(HCit)_2^-$	**$Ca(Cit)^-$** Ca(HCit) $Ca(H_2Cit)^+$	$Ca_3(Cit)_2{:}4H_2O_{(s)}$
Am(III)	ISA	**$Am(OH)_3(HISA)^-$**	**Ca(ISA)** Ca(HISA)+	$Ca(HISA)_{2(cr)}$
Eu(III)	ISA	**$Eu(OH)_3(HISA)^-$**	**Ca(ISA)** Ca(HISA)+	$Ca(HISA)_{2(cr)}$
Th	ISA	**$CaTh(OH)_4(HISA)^+$** $Th(OH)_4(HISA)^-$ $Th(OH)_4(HISA)_2^{2-}$ $Th(OH)_3(HISA)$ $Th(OH)_3(HISA)_2^-$	**Ca(ISA)** Ca(HISA)+ $CaTh(OH)^4(HISA)^+$	$Ca(HISA)_{2(cr)}$
Th	NTA	$Th(NTA)^+$ Th(OH)(NTA) **$Th(OH)_2(NTA)^-$**	**$Ca(NTA)^-$** Ca(HNTA) $Ca(HNTA)_2^{2-}$	
Th	Citrate	$Th(Cit)^+$ **$Th(Cit)_2^{2-}$**	**$Ca(Cit)^-$** Ca(HCit) $Ca(H_2Cit)^+$	$Ca_3(Cit)_2{:}4H_2O_{(s)}$

The first calculations examined changes in speciation during the titration and were used to assess whether the thermodynamic speciation calculations were in general agreement with the effects on sorption observed by Dario et al. (2004). The second calculations provided insight into the ability of the complexing agent to influence sorption at portlandite concentrations representative of SFR.

A3.3 Results and discussion

A3.3.1 Am(III) and NTA

In the PhreeqC calculations of Dario's experimental conditions, the concentration of $Ca(NTA)^-$ increased until all Ca^{2+} in the system, i.e. in the portlandite, was complexed (Figure A3-3). Once all Ca had been complexed, Am(III) was complexed rapidly by the NTA added. The pH of the modelled system was affected by the addition of NTA but was pH 12.6 at the point where rapid Am complexation occurred, which is relevant to portlandite-buffered conditions. Furthermore, the $AmNTA_2^{3-}$ species dominates Am speciation in the pH range of pH 6–13, as shown in a titration calculated with 0.001 M NTA and 10^{-8} M Am (100 % from pH 6 to 12.8, 99.9 % at pH 13.0).

The pattern observed, that NTA has an immediate and strong effect on trivalent actinide speciation once all Ca^{2+} is complexed, agrees well with the effect on sorption observed by Dario et al. (2004).

In the model of concrete porewater, which equilibrated to pH 12.9, the titration of NTA resulted in continued complexation of Ca^{2+}, which was provided by the portlandite, and had a limited effect on Am speciation. With 1×10^{-2} M NTA added, only 0.01 % of the Am(III) was present as an NTA species.

In Dario's experiments, 1×10^{-2} M NTA reduced the long term K_d of Eu(III) by two orders of magnitude. The PhreeqC calculations of his experiments suggest that all of the Eu(III) was complexed by NTA. Therefore, when the PhreeqC calculations suggest that only 0.01 % of Am is complexed by 10 mM NTA in concrete porewater, NTA is not expected to affect the sorption of trivalent actinides significantly.

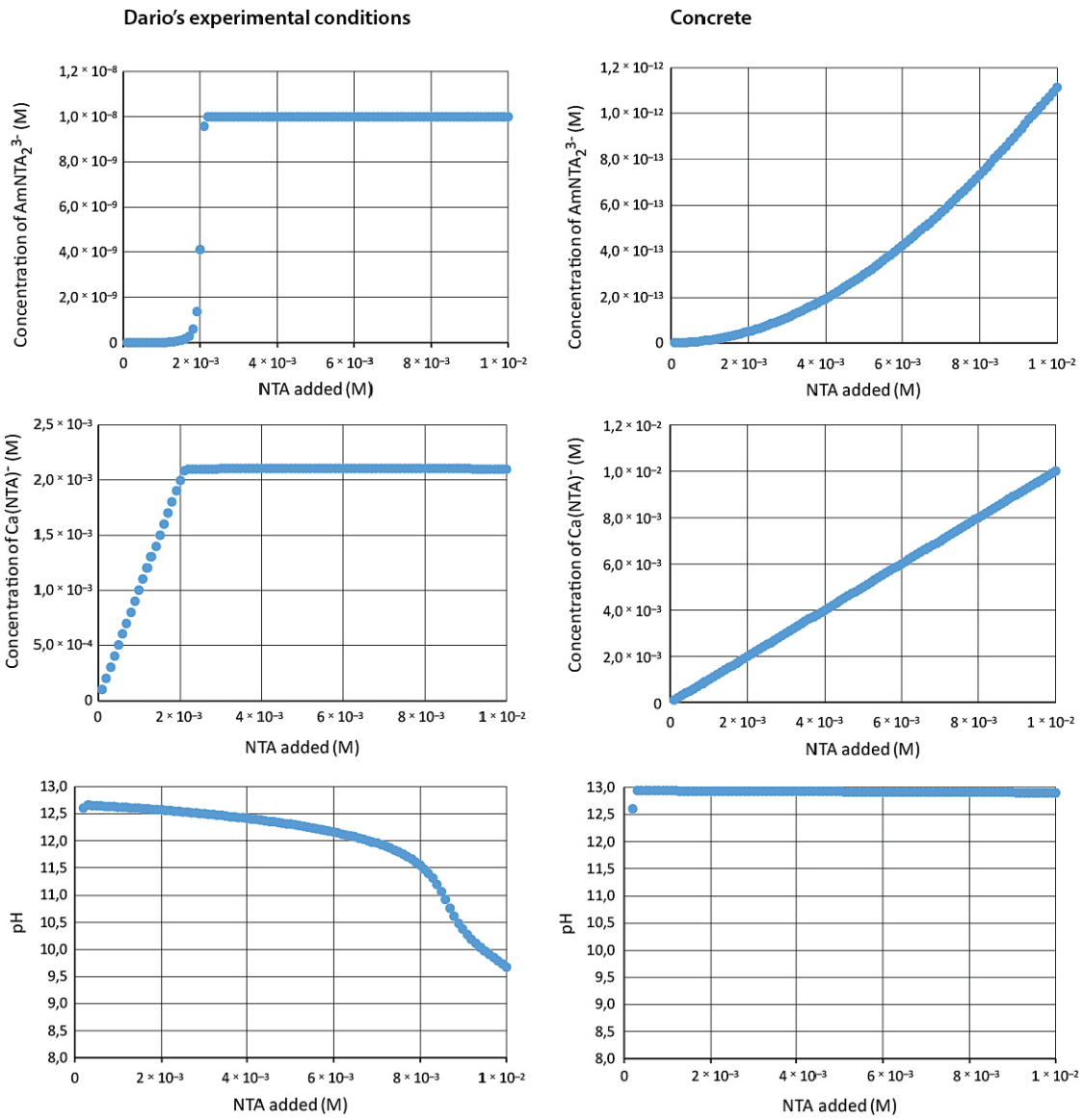

Figure A3-3. *Concentrations of $AmNTA_2^{3-}$ (top row), $CaNTA^-$ (middle row) and pH (bottom row) in PhreeqC calculations representative of the experimental conditions in Dario et al. (2004) (left hand column) and in concrete porewater (right hand column). Note that $AmNTA_2^{3-}$ and $CaNTA^-$ are the only NTA complexes visible on the scale used. Am(III) is present as a mixture of hydroxide complexes (not shown) when it is not present as an NTA complex.*

A3.3.2 Am(III) and citrate

Without precipitation of Ca_3Cit_2

In the PhreeqC model of Dario's experimental conditions, the concentration of $Ca(Cit)^-$ increased until all Ca in the system, i.e. in the portlandite, was complexed (Figure A3-4). Although the pattern is similar to that seen with Ca and NTA, the interaction between Ca and citrate was weaker. This resulted in a < 1:1 increase in the $Ca(Cit)^-$ concentration as citrate was added. The calculated pH decreased as citrate was added, and had reached pH 12.4 when Am-citrate species began to form significantly (4 mM citrate added) and pH 11.5 by the point maximum Am complexation by citrate was reached (8 mM citrate).

Simple Am(III)-citrate pH titration calculations with 10^{-8} M Am(III) and 1 or 10 mM citrate (Figure A3-5) show that the formation of Am(III)-citrate species is very sensitive to pH in this pH range. The concentrations of Am(III)-citrate complexes decrease as the pH increases, particularly with the lower citrate concentration investigated. Am(III) forms hydroxy complexes, such as $Am(OH)_4^-$, preferentially at high pH. Note that precipitation of $Am(OH)_3$ was not included in the calculations.

The pH control can explain the delay seen in the calculated formation of Am(III)-citrate species once all Ca^{2+} had been complexed (Figure A3-1), and the slow increase in Am(III)-citrate species from this point.

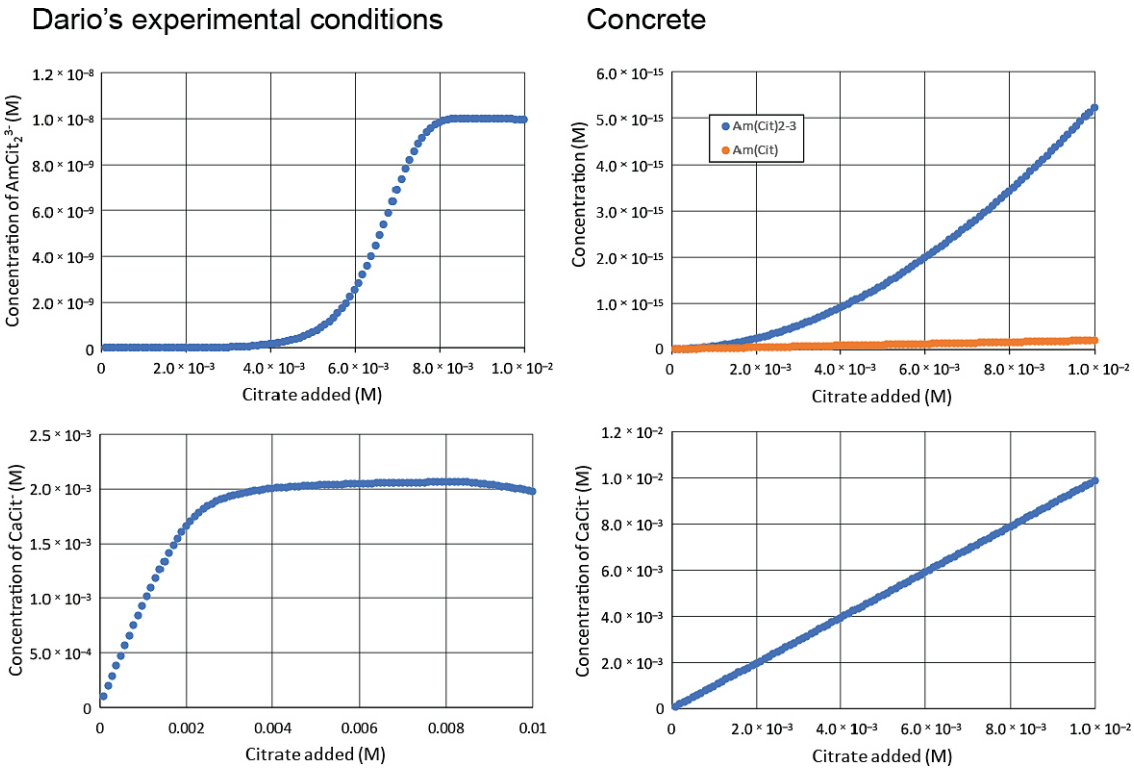

Figure A3-4. *Concentrations of $AmCit_2^{3-}$ (top row) and $CaCit^-$ (bottom row) in PhreeqC calculations representative of the experimental conditions in Dario et al. (2004) (left hand column) and in concrete porewater (right hand column), without precipitation of $Ca_3Citrate_2$. Note that under Dario's experimental conditions, $AmCit_2^{3-}$ and $CaCit^-$ are the only citrate complexes visible on the scale used. Am(III) is present as as a mixture of hydroxide complexes (not shown) when it is not present as a citrate complex.*

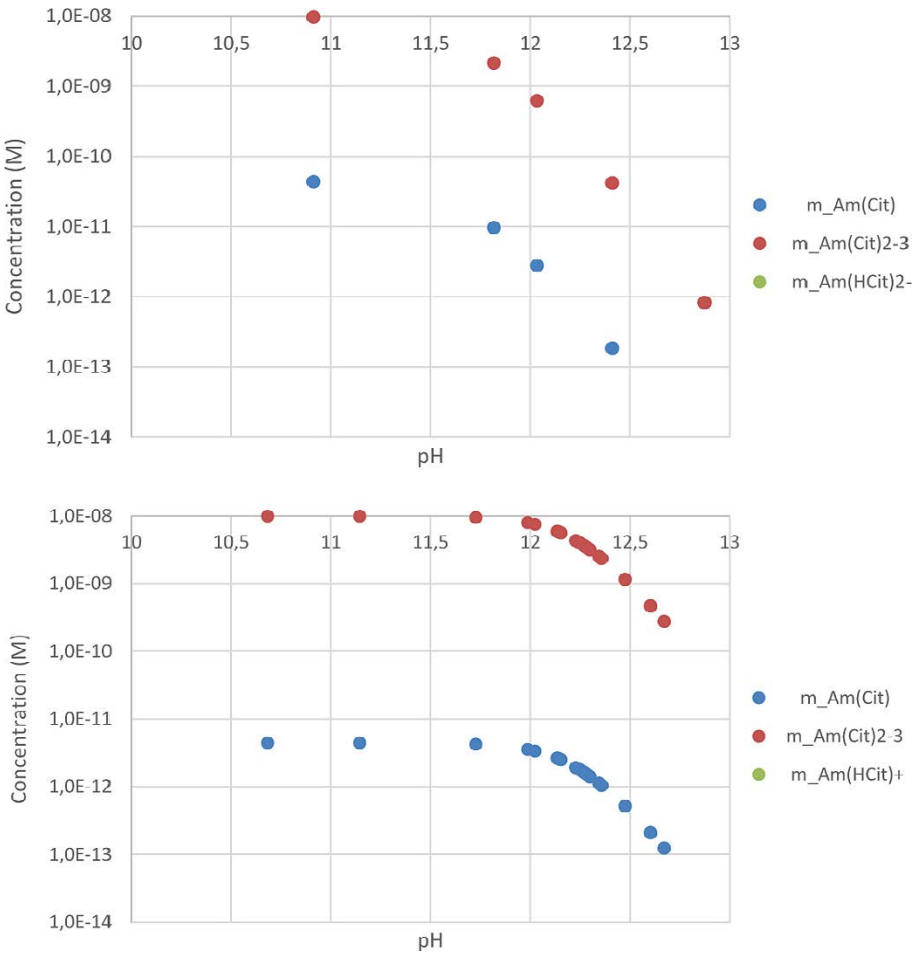

Figure A3-5. *Concentration of Am(III)-citrate species in a solution of 1×10^{-8} M Am(III) and a) 1 mM citrate and b) 10 mM citrate, as a function of pH in the region pH 10–13. Am(III) is present as as a mixture of hydroxide complexes (not shown) when it is not present as a citrate complex.*

The results of the calculation are in general agreement with the observed experimental effect of citrate on Eu(III) sorption in Dario et al. (2004). Eu(III) complexation was not observed until all Ca^{2+} was complexed, and the effect from this point was more gradual than the effect of NTA. The pH of the experiments also decreased as citrate was added, although not to the extent calculated in the PhreeqC model of the experiments. With 10 mM citrate the experimental pH was 12.13 compared to pH 12.54 with 0.3 mM citrate. PhreeqC calculations suggest that about 60 % of Eu(III) would be complexed by 10 mM citrate in a simple pH 12.13 solution, compared to 0.021 % of Eu(III) in a 0.3 mM citrate solution at pH 12.53. Therefore, the trend of reduced sorption with increased citrate observed in the experiments appears to reflect an increased concentration of Eu-citrate complexes both due to the increased concentration of available citrate and the decrease in experimental pH.

In the calculations of concrete porewater (pH 12.9), the dissolution of portlandite resulted in the on-going formation of Ca-citrate species, while Am(III)-citrate complexes comprised a tiny fraction of the total Am species. In a simple pH 12.5 solution with 10 mM citrate and no Ca^{2+}, PhreeqC predicts that ~1 % of the Am(III) is complexed. Therefore, both the pH and the high Ca^{2+} concentration contribute to the limited complexation of Am(III).

With precipitation of Ca_3Cit_2

Precipitation of Ca_3Cit_2 did not occur in the calculations representing Dario's experimental conditions.

In the model of concrete porewater, the increase in dissolved $Ca(Cit)^-$ concentration stopped following the addition of 1.3×10^{-3} M citrate, when $Ca_3Cit_{2(s)}$ precipitation started (Figure A3-6). Once $Ca_3Cit_2(s)$ precipitation had started, no further Am(III)-Cit complexes formed as citrate was added.

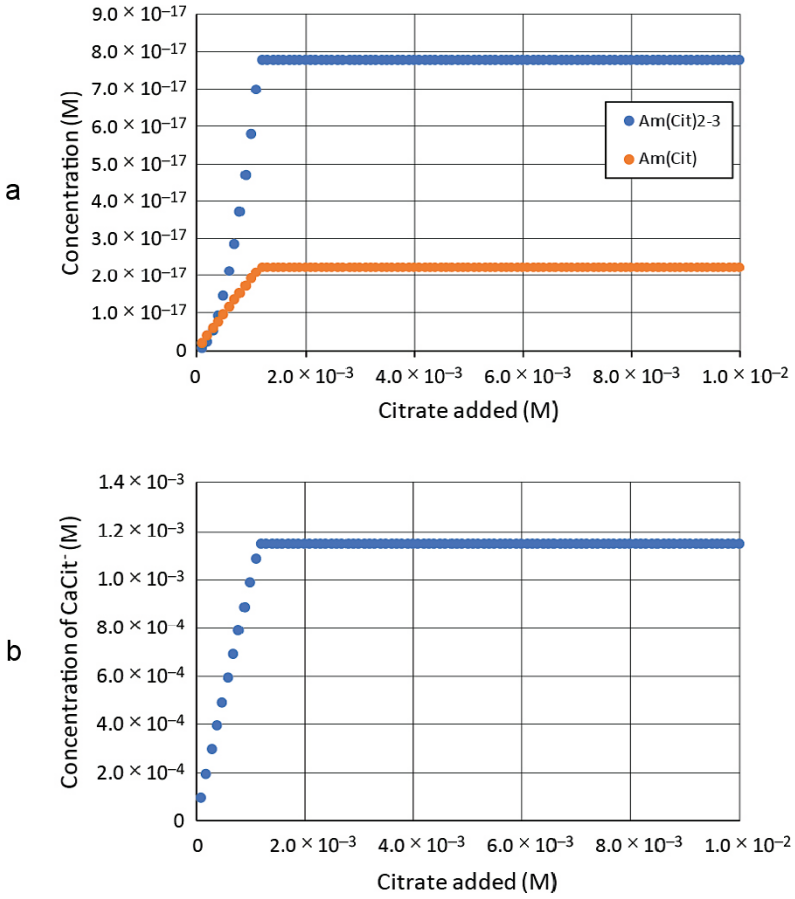

Figure A3-6. *Formation of a) Am(III)-citrate species and b) $CaCit^-$ in concrete porewater as a function of citrate added (pH 12.9), allowing for precipitation of Ca_3Cit_2. Note that Am(III) is present as as a mixture of hydroxide complexes (not shown) when it is not present as a citrate complex).*

Conclusions relating to Am and citrate

The PhreeqC calculations indicate that:

- citrate concentrations will be limited to ~1 mM by the presence of portlandite in SFR.
- only a small proportion of Am(III) is complexed by 1 mM citrate at pH 12.5 in the absence of Ca^{2+}.
- citrate available for Am(III) complexation will be further reduced by the formation of Ca-citrate complexes, with Ca^{2+} supplied by portlandite.
- citrate complexation of Am(III) is not relevant in SFR.

A3.3.3 Am(III) and ISA

The concentrations of $CaHISA^+$ and CaISA were calculated to increase as ISA was added, but the gradient of the line was much less than 1 (Figure A3-7). This indicates a weaker interaction than seen for Ca^{2+} with NTA or citrate. Complexation of Am(III) was therefore calculated to occur with lower concentrations of ISA than other ligands. 98.5 % of the Am was complexed when the first step of the titration (1×10^{-4} M ISA) was complete. This is generally consistent with the experimental results of Dario et al. (2004), which showed that Ca^{2+} had no observable influence on the effect of ISA on Am(III) sorption to cement and TiO_2. The addition of 10^{-2} M ISA only reduced the calculated pH from pH 12.7 to 12.4, and a simple pH titration with 0.001 M ISA and 10^{-8} M Am showed that $Am(OH)_3(HISA)^-$ consistently comprises > 99.9 % of the Am species above pH 11.7.

The relatively weak Ca-ISA interaction was seen again in the concrete porewater calculations, although the higher available Ca concentration pushes the equilibrium towards complex formation. In this calculation, 94 % of the Am was complexed when the first step of the titration (1×10^{-4} M ISA) was complete.

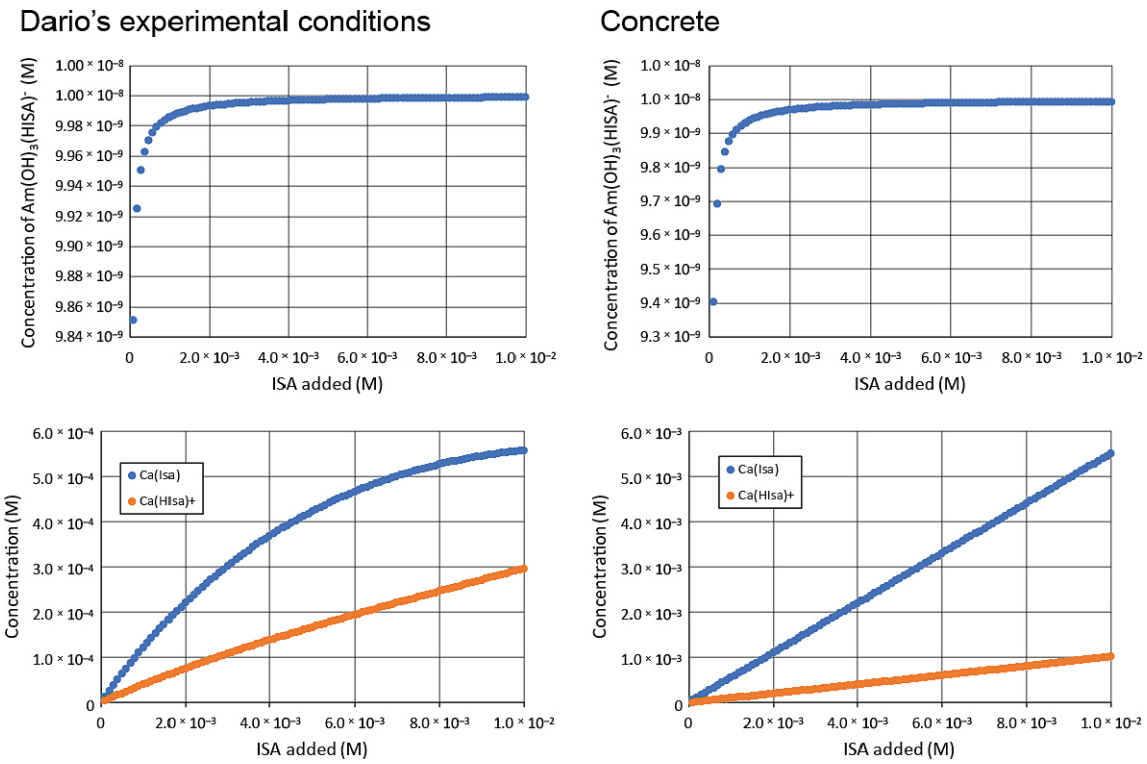

Figure A3-7. *Concentrations of $Am(OH)_3(HISA)^-$ (top row) and Ca(II)-ISA species (bottom row) in PhreeqC calculations representative of the experimental conditions in Dario et al. (2004) (left hand column) and in concrete porewater (right hand column). Note that $Am(OH)_3(HISA)^-$ is the only Am-ISA species in the database. Am(III) is present as as a mixture of hydroxide complexes (not shown) when it is not present as $Am(OH)_3(HISA)^-$.*

Comparison with Eu(III)-ISA

The trend for $Eu(OH)_3(HISA)^-$ was very similar to that of $Am(OH)_3(HISA)^-$ (results not shown), but the slightly higher stability constant resulted in 98.9 % of the Eu(III) being present as $Eu(OH)_3(HISA)^-$ in concrete porewater when the first step of the ISA titration (1×10^{-4} M ISA) was complete, compared to 94 % with Am(III). This gives confidence that it is reasonable to compare PhreeqC calculations using Am(III) with the Eu(III) experimental results.

Th(IV) ISA, NTA and citrate

Hydrolysed Th(IV)-ISA and -NTA species were found to dominate Th(IV) speciation under alkaline conditions, notably $CaTh(OH)_4(HISA)^+$ and $Th(OH)_2(NTA)^-$. In the concrete system, 100 % of the Th(IV) was complexed by 0.01 M ISA and NTA. Even after the first step of the titration (1×10^{-4} M complexing agent), 99.7 % and 100 % of the Th was calculated to be complexed by ISA and NTA, respectively.

The results contrast with the results of Hummel (1993), which suggested that NTA is not able to complex Th(IV) in cement porewater. The different results probably reflect improvements in the understanding of actinide speciation under highly alkaline conditions and the thermodynamic data available.

Citrate was not found to form complexes with Th(IV) under concrete porewater conditions. As seen for Am(III) and citrate, Th-citrate complexes do not form to any significant degree at highly alkaline pH due to the preferential formation of hydroxy complexes, mainly $Th(OH)_4$. Note that precipitation of $Am(OH)_3$ and $Th(OH)_4$ was not included in the calculations.

A3.4 Discussion and conclusions

General agreement between the results of Dario et al. (2004) and the calculations with Am(III) representing the experimental conditions gives confidence in the speciation predicted for trivalent actinides. The results of the thermodynamic calculations are summarized in Table A3-2.

In the cases where an actinide was calculated to be complexed significantly by organic complexing agents under SFR conditions, the dominant species involved hydroxo ligands ($Am(OH)_3(HISA)^-$, $Eu(OH)_3(HISA)^-$, $CaTh(OH)_4(HISA)^+$ and $Th(OH)_2(NTA)^-$). The ability to form this type of mixed ligand complex therefore appears to be important for the complex to form under SFR conditions.

Table A3-2. Summary of the PhreeqC calculations.

Radionuclide	Complexing agent	Fraction radionuclides complexed with 0.01 M complexing agent and 1 g/L cement (%)	Fraction radionuclides complexed in concrete porewater with 0.01 M complexing agent (%)	Comment
Am	NTA	100	0.01	No effect in SFR
Am	Citrate	100 (pH 9.9)	< 0.001	No effect in SFR
Am	ISA	100	100	Am-OH-ISA species; 94 % Am complexation with 1×10^{-4} M ISA in concrete porewater
Eu	ISA	100	100	Eu-OH-ISA species; 98.9 % Eu complexation with 1×10^{-4} M ISA in concrete porewater
Th	ISA	100	100	Th-OH-ISA species; 99.7 % Th complexation with 1×10^{-4} M ISA in concrete porewater
Th	NTA	100	100	Th-OH-NTA species; 100 % Th complexation with 1×10^{-4} M ISA in concrete porewater
Th	Citrate		0	No effect in SFR

Appendix 4

ISA concentration data for different time periods

Table A4-1. Concentrations of ISA (M) over time for each relevant part of SFR, based on the degradation of cellulose over time and considering sorption to all available hydrated cement.

Time (a)	10	100	500	1 000	5 000
1BMA: compartment					
1	0	0	0	0	0
2	2.2×10^{-6}	6.3×10^{-6}	2.2×10^{-5}	3.5×10^{-5}	6.0×10^{-5}
3	1.9×10^{-6}	5.4×10^{-6}	1.9×10^{-5}	3.0×10^{-5}	5.1×10^{-5}
4	4.1×10^{-6}	1.2×10^{-5}	4.2×10^{-5}	6.9×10^{-5}	1.2×10^{-4}
5	1.1×10^{-7}	3.0×10^{-7}	1.0×10^{-6}	1.6×10^{-6}	2.6×10^{-6}
6	5.6×10^{-7}	1.6×10^{-6}	5.3×10^{-6}	8.5×10^{-6}	1.4×10^{-5}
7	2.6×10^{-6}	7.6×10^{-6}	2.6×10^{-5}	4.2×10^{-5}	7.4×10^{-5}
8	7.0×10^{-6}	2.0×10^{-5}	7.4×10^{-5}	1.3×10^{-4}	2.5×10^{-4}
9	6.5×10^{-6}	1.9×10^{-5}	6.8×10^{-5}	1.2×10^{-4}	2.2×10^{-4}
10	7.0×10^{-6}	2.0×10^{-5}	7.3×10^{-5}	1.3×10^{-4}	2.4×10^{-4}
11	1.0×10^{-5}	2.9×10^{-5}	1.1×10^{-4}	2.0×10^{-4}	4.2×10^{-4}
12	4.6×10^{-8}	1.3×10^{-7}	4.3×10^{-7}	6.9×10^{-7}	1.1×10^{-6}
13	0	0	0	0	0
14	0	0	0	0	0
15	0	0	0	0	0
Total 1BMA construction	3.6×10^{-6}	1.0×10^{-5}	3.6×10^{-5}	5.9×10^{-5}	1.1×10^{-4}
1BMA vault incl. macadam and shotcrete	3.5×10^{-6}	9.9×10^{-6}	3.4×10^{-5}	5.7×10^{-5}	1.0×10^{-4}
2BMA					
2BMA per caisson	6.8×10^{-7}	1.9×10^{-6}	6.5×10^{-6}	1.0×10^{-5}	1.7×10^{-5}
2BMA vault	5.4×10^{-7}	1.5×10^{-6}	5.2×10^{-6}	8.3×10^{-6}	1.4×10^{-5}
Silo					
Silo construction	6.7×10^{-7}	1.9×10^{-6}	6.4×10^{-6}	1.0×10^{-5}	1.7×10^{-5}
Entire vault	6.6×10^{-7}	1.9×10^{-6}	6.4×10^{-6}	1.0×10^{-5}	1.7×10^{-5}
1BTF					
Waste zone	2.3×10^{-8}	6.4×10^{-8}	2.1×10^{-7}	3.4×10^{-7}	5.7×10^{-7}
Entire vault	2.2×10^{-8}	6.2×10^{-8}	2.1×10^{-7}	3.3×10^{-7}	5.4×10^{-7}

Arkitektkopia AB, Bromma, 2021

SKB is responsible for managing spent nuclear fuel and radioactive waste produced by the Swedish nuclear power plants such that man and the environment are protected in the near and distant future.

skb.se